THE LIQUID STATE OF MATTER: Fluids, Simple and Complex
E.W. Montroll and J.L. Lebowitz (editors)

Low Frequency Dielectric Properties of Liquid and Solid Water

Frank H. Stillinger
Bell Telephone Laboratories
Murray Hill, New Jersey U.S.A. 07974

I. INTRODUCTION

One of the primary reasons that water is important to us is its ability to serve as a solvent. That ability stems in large part from its high dielectric constant. This chapter is devoted to clarifying the logical connections between the molecular structure of water, the manner in which intermolecular forces cause water molecules to aggregate in condensed phases, and the response of those phases to external electrical fields. The last of these defines the dielectric properties.

This survey will be restricted to pure water in liquid and solid forms. With respect to the latter, only those polymorphs of ice which can be prepared under ordinary pressures, namely hexagonal ice Ih and the cubic modification Ic, will be considered. Furthermore only linear dielectric response will be studied. But even with these restrictions the subject is a rich one containing several theoretical subtleties and many important phenomena.

We begin this review in Section II with a brief outline of the relevant measurements. A comprehensive understanding of these measurements for liquid and solid water is an indispensable prerequisite to motivate and to guide development of the subsequent theory.

Section III initiates the molecular theory with a discussion of several general issues that are applicable to all phases of water. One of these issues is the identification of a formal procedure for assigning multipole moments to molecules, a nontrivial matter

when electron distributions from neighboring molecules overlap. Another matter of general importance covered in Section III is the definition of molecular distribution functions and an exposition of their basic properties.

After having explored these few generally applicable ideas it has seemed advisable to treat liquid water, and the ices, as separate topics. These two cases present rather distinct statistical problems, and the dielectric behaviors at the molecular level respectively are clearly different. Consequently the discussion of bulk liquid water is contained in Section IV, while Section V then considers the interesting and complex problems presented by ices Ih and Ic.

Although most of the conceptual aspects of the theory now seem well in hand there still remain several important quantitative problems to be resolved. These are highlighted in the following development. It is the author's hope that the present survey will stimulate activity that soon closes these gaps in our understanding.

For those readers interested in a broader treatment of the subject of aqueous dielectrics, the recent book by Hasted (1973) is recommended as a suitable guide.

II. DIELECTRIC MEASUREMENTS

A. Background and Definitions

The macroscopic electrical behavior of isotropic dielectric substances is characterized by the scalar dielectric constant ϵ. This quantity serves as the proportionality constant in the linear relation between the electric field **E** and the dielectric displacement **D**.

$$\mathbf{D} = \epsilon\,\mathbf{E}\ . \tag{2.1}$$

It is often useful to consider as well the polarization vector **P** which is related to ϵ and **E** by the following expression:

$$\mathbf{P} = (\epsilon-1)\mathbf{E}/4\pi\ . \tag{2.2}$$

Liquid water and cubic ice as bulk phases are both dielectrically isotropic, so for them the scalar ϵ description is appropriate. The same is probably true for the amorphous solid deposits that have been formed by slow condensation of water vapor on very cold surfaces (Narten *et al.* 1976). However ordinary hexagonal ice Ih has lower symmetry, so that its dielectric response demands use of a dyadic tensor quantity ϵ; Eq. (2.1) then becomes

$$\mathbf{D} = \epsilon\cdot\mathbf{E} \tag{2.3}$$

and Eq. (2.2) must be modified accordingly:

$$\mathbf{P} = (\epsilon-\mathbf{1})\cdot\mathbf{E}/4\pi\ . \tag{2.4}$$

Hexagonal ice requires two independently specified tensor components of ϵ describing respectively the response to electrical fields oriented parallel to the hexagonal c axis, and perpendicular to that axis (*i.e.* in the basal plane). In a Cartesian coordinate system x,y,z with the z axis coincident with the hexagonal c axis, the dielectric tensor is diagonal and has the form

$$\epsilon = \begin{pmatrix} \epsilon_b & 0 & 0 \\ 0 & \epsilon_b & 0 \\ 0 & 0 & \epsilon_c \end{pmatrix} \tag{2.5}$$

Similar remarks apply to the case of water at interfaces. Liquid water at a planar interface, such as the liquid-vapor surface or the region near a planar electrode, can be expected to manifest tensor dielectric behavior with separate normal (ϵ_N) and tangential (ϵ_T) components. Boundaries with two distinct curvatures generally will produce three independent tensor components. In any case the dielectric tensor is symmetrical and can be diagonalized by a suitable choice of local coordinates.

Dielectric constants have values that depend on the angular frequency ω of the per-

turbing field, and it has long been realized that these ω variations contain important information about dynamics of molecular processes occurring in the materials of interest. Generally dielectric response will lag the excitation, giving rise to energy dissipation. Within the linear response regime it is conventional to separate $\epsilon(\omega)$ into real (ϵ') and imaginary (ϵ'') parts as follows:

$$\epsilon(\omega) = \epsilon'(\omega) - i\epsilon''(\omega) . \tag{2.6}$$

[Similar representations are appropriate for each component of a tensor ϵ.]

The principle of causality demands that electrical response never precede the excitation. This obvious requirement translates into a mathematical connection between ϵ' and ϵ'', the Kramers-Kronig equations (Kittel 1958).

$$\epsilon'(\omega) - \epsilon'(\infty) = \frac{2}{\pi} \int_0^\infty \frac{u\epsilon''(u)}{u^2 - \omega^2} du , \tag{2.7}$$

$$\epsilon''(\omega) = -\frac{2\omega}{\pi} \int_0^\infty \frac{\epsilon'(u) - \epsilon'(\infty)}{u^2 - \omega^2} du .$$

Cauchy principal values are to be taken in these integrals at the poles of the integrands along the positive real axis. Notice the "infinite frequency" subtraction for ϵ'; for most cases of practical importance "infinite frequency" can be construed to lie above the characteristic frequency range of molecular vibrations but below the frequency range of molecular electronic transitions. The two Kramers-Kronig relations are inverse integral transforms to one another (specifically, modified Hilbert transforms) and so constitute only a single independent functional connection between the two quantities involved.

As announced in the Introduction, this review will be concerned with the low frequency limit. In the case of perfectly insulating dielectrics we can simply observe that

$$\lim_{\omega \to 0} \epsilon'(\omega) = \epsilon_0 > 1 , \tag{2.8}$$

$$\lim_{\omega \to 0} \epsilon''(\omega) = 0 ,$$

and ϵ_0 is the standard static dielectric constant. However water does not fit this ideal description. Even in pure form it is electrically conducting owing to formation of ions by the reversible dissociation reaction

$$H_2O \rightleftharpoons H^+ + OH^- . \tag{2.9}$$

In liquid water at 20°C the concentration of these ions is only 8.3×10^{-8} moles/l, but they have exceptionally high mobilities and thus might tend to interfere with high precision measurement of the static dielectric constant (Stillinger 1978).

If σ represents the low-frequency conductivity then in the neighborhood of $\omega = 0$ the imaginary part of $\epsilon(\omega)$ diverges thus:

$$\epsilon''(\omega) = (4\pi\sigma/\omega) + O(\omega) . \tag{2.10}$$

In order for this form to emerge from the second of the Kramers-Kronig relations (2.7) it is necessary for ϵ' to possess a delta-function divergence at zero frequency:

$$\epsilon'(\omega) = 4\pi^2\sigma\,\delta(\omega) + \epsilon_0 + O(\omega^2) . \tag{2.11}$$

The physical meaning of this leading term is simply that a conductor can completely shield its interior from external electric fields. For practical reasons ϵ' is always measured at nonzero frequency so that in principle the delta function is not encountered; in practice of course the nonzero conductivity can create troublesome space-charge buildup within a measurement apparatus and thus lead to spurious results unless suitable precautions are observed.

B. Observed Static Dielectric Constants

Malmberg and Maryott (1956) have made one of the most precise measurements of the static dielectric constant for liquid water over its normal temperature range 0°-100°C. To within a claimed maximum uncertainty of ± 0.05 their results could be fitted to the following cubic polynomial:

$$\epsilon_0 = 87.740 - 4.008\times10^{-1}t + 9.398\times10^{-4}t^2 - 1.410\times10^{-6}t^3 , \qquad (2.12)$$

where t is the Celsius temperature. This function is monotonically decreasing from 0°C to 100°C, reaching a value 55.648 at the upper limit, the normal boiling point of water. Although some of the reduction in ϵ_0 with rising temperature may be attributed to decreasing density, that is only part of the explanation, for in the neighborhood of 4°C where the thermal expansion of the liquid vanishes ϵ_0 is decreasing with temperature.

In order to follow liquid water along the saturation line to the critical point (374.15°C) it is of course necessary to go to elevated pressure. Akerlof and Oshrey (1950) find that between 100°C and 370°C along this saturation line

$$\epsilon_0 = 5321/T + 233.76 + 9.297\times10^{-1}T + 1.417\times10^{-3}T^2 - 8.292\times10^{-7}T^3 \qquad (2.13)$$

where T is the absolute temperature in °K. This expression shows a continuation of the downward trend of ϵ_0 for liquid water with rising temperature.

The Akerlof-Oshrey formula cannot be expected to represent ϵ_0 faithfully right up to the critical point. Nor can any analogous expression involving rational functions of T be expected to do so. Owing to the peculiar "nonclassical" nature of the critical point in fluids (Stanley, 1971) we must expect ϵ_0 along the saturation line to have an expression of the form

$$\epsilon_0 = \epsilon_c + A_1(T_c - T)^{p_1} + A_2(T_c - T)^{p_2} + \ldots \qquad (2.14)$$

where T_c is the critical temperature, the A_i are suitable constants, and the p_i are fractional exponents. At present no critical region measurements on any polar fluid are available with the precision necessary to determine even the leading correction term parameters A_1 and p_1, and this remains an important open area for future investigation. The critical dielectric constant ϵ_c is the common limit for coexisting liquid and vapor dielectric constants, and from measurements quoted by Franck (1970) it is possible to infer that

$$\epsilon_c \cong 6.0 \qquad (2.15)$$

In this critical state the mass density of water is only 0.32g/cm^3.

Owen *et al.* (1961) determined the pressure coefficient of ϵ_0 for water within its normal liquid range. Their results show that isothermal compression increases ϵ_0. Specifically they found

$$(\partial \ln\epsilon_0/\partial p)_T = 4.51\times10^{-5}/\text{bar} \quad (0°C) \qquad (2.16)$$
$$= 5.24\times10^{-5}/\text{bar} \quad (70°C)$$

with smooth and monotonic behavior between these extreme temperatures of observation.

The static dielectric constant of liquid D_2O has been measured by Malmberg (1958). Over the temperature range 4°C to 100°C his results could be represented by the following cubic polynomial:

$$\epsilon_0(D_2O) = 87.482 - 4.0509\times10^{-1}t + 9.638\times10^{-4}t^2 - 1.333\times10^{-6}t^3 , \qquad (2.17)$$

where again t is in °C. At any given temperature for which both formulas apply, Eq. (2.12) for $\epsilon_0(H_2O)$ gives slightly larger values than Eq. (2.17) for $\epsilon_0(D_2O)$.

The properties of strongly supercooled water have offered some interesting surprises that could not have been reasonably anticipated by simply extrapolating fitted data in the normal liquid range to low temperature. As Angell and his collaborators have stressed (Speedy and Angell, 1976) supercooled water behaves as though it possessed an order-disorder transition, or lambda anomaly, at T_s=−45°C. Since the homogeneous nucleation temperature for freezing lies at about -40°C, this apparent higher-order transition has never actually been reached. Nevertheless its existence is revealed by the singular behavior of various measurable properties. Fractional power formulas analogous to that quoted above [Eq. (2.14)] appear to be applicable, with

some properties (such as the isothermal compressibility) actually diverging at T_s.

Hodge and Angell (1978) have examined ϵ_0 for supercooled water (in emulsified form) to -35°C. They found it possible to represent their measurements by the simple expression

$$\epsilon_0 = A[(T/T_s)-1]^{\gamma} , \tag{2.18}$$

where T is in °K and

$$A = 72.94 \ , \ T_s = 228°K, \ \gamma = -0.1256 \ . \tag{2.19}$$

The negative exponent γ indicates a weak divergence to infinity at the singular point T_s. Studies of supercooled water at elevated pressure (Kanno and Angell, 1979) suggest that if expression (2.18) remains valid under compression, T_s must decrease with increasing pressure.

As liquid water at 0°C freezes to form hexagonal ice it is generally agreed that the dielectric constant increases discontinuously. Unfortunately there is disagreement about the anisotropy of the dielectric tensor in this crystal. Humbel, Jona, and Scherrer (1953) find at -10°C that

$$\epsilon_b = 95 \ , \ \epsilon_c = 111 \ , \tag{2.20}$$

with both components increasing as temperature declines. On the other hand Auty and Cole (1952) have found for *polycrystalline* ice [for which ϵ_0 should be close to $(2\epsilon_b+\epsilon_c)/3$] that the apparent dielectric constant is close to ϵ_b alone from the Humbel, Jona, and Scherrer work. More recently Wörz and Cole (1969) and Johari and Jones (1978) report failure to uncover any significant anisotropy. The first pair of this latter group of authors find that the following equation represents their measurements:

$$\epsilon_0-\epsilon_\infty = 20715/(T-T_0) \ , \tag{2.21}$$

wherein

$$\epsilon_\infty = 3.1 \ , \ T_0 = 38°K \ . \tag{2.22}$$

The temperature T_0 thus plays the role of a formal Curie temperature, suggesting that if indeed accurate measurements could be made to below T_0 hexagonal ice would become ferroelectric. This latter possibility has been discussed by Onsager (1967).

It seems safe to say that hexagonal ice has little, if any, anisotropy. On symmetry grounds it is impossible to believe that $\epsilon_b-\epsilon_c$ precisely vanishes at all temperatures. However a convincing measurement of this anisotropy remains for the future.

No measurements are available for ϵ_0 in cubic ice. The difficulty concerns the low temperature required by this polymorph for stability ($T \lesssim 150°K$), and the resulting extreme sluggishness of electrical relaxation processes.

C. Water Molecule

Ultimately it must be the electrical properties of individual water molecules that cause macroscopic dielectric behavior of the bulk substances. Therefore we list here a few pertinent parameters that have been measured for the individual water molecule.

In its ground electronic state the molecule has C_{2v} symmetry. The covalent OH bonds have length 0.9584Å, and are arranged at bond angle 104.45° (Kern and Karplus, 1972).

The most important attribute displayed by the water molecule is its dipole moment μ. Dyke and Muenter (1973) have found that

$$|\mu| = 1.855\times10^{-13} \text{ esu cm} \ . \tag{2.23}$$

Of course the vector moment is directed along the symmetry axis with its negative end at the oxygen atom end its positive and pointing between the hydrogen atoms. By combining this moment with the above molecular geometry it is possible to assign partial charges to the H and O atoms as a rough electrical description of the water molecule; one obtains 0.3289*e* and -0.6578*e* for H and O respectively, where *e* is the

bare proton charge.

The mean electronic polarizability of the molecule has been extracted from vapor-phase refractive index measurements, and has the value (Eisenberg and Kauzmann, 1969)

$$\bar{\alpha} = 1.444\times10^{-24}\text{cm}^3 \, . \tag{2.24}$$

In principle the polarizability in anisotropic, with three independent tensor components. No experimental measurements of the separate components exist. However Liebmann and Moskowitz (1971) have carried out accurate Hartree-Fock computations which give the separate components

$$\begin{aligned} \alpha_{11} &= 1.452\times10^{-24}\text{cm}^3 \\ \alpha_{22} &= 1.651\times10^{-24}\text{cm}^3 \\ \alpha_{33} &= 1.226\times10^{-24}\text{cm}^3 \end{aligned} \tag{2.25}$$

whose average, $1.443\times10^{-24}\text{cm}^3$, is very close to $\bar{\alpha}$ in Eq. (2.24). Subscripts 1, 2, and 3 in Eq. (2.25) refer to principal directions; the first is along the symmetry axis of the molecule, the second in the molecular plane but perpendicular to the symmetry axis, and the third is perpendicular to the molecular plane.

The electrical quadrupole tensor measures second spatial moments of $\rho_e(\mathbf{r})$, the electrostatic charge density of the molecule. This density comprises contributions both from the nuclear point charges as well as from the continuous and extended electron cloud. The elements of the traceless quadrupole tensor are defined thus:

$$\Theta_{ij} = \tfrac{1}{2} \int \left(3x_i x_j - r^2\right) \rho_e(\mathbf{r}) d\mathbf{r} \, . \tag{2.26}$$

In the case of a molecule such as water which possesses a permanent dipole moment, these tensor elements depend upon the choice of origin for the coordinate system.

Verhoeven and Dymanus (1970) have measured the electrical quadrupole tensor

for D_2O by molecular beam Zeeman spectroscopy. Presumably the results (in a common coordinate system) would be nearly the same for H_2O. The natural coordinate origin in such experiments is the molecular center of mass. From the point of view of the present study it is more convenient instead to place the coordinate origin at the oxygen nucleus. After applying the required transformation to the results of Verhoeven and Dymanus (Stillinger, 1975) the quadrupole moments are found to be

$$\begin{aligned} \Theta_{11} &= 0.116\times10^{-26} \text{ esu cm}^2 \\ \Theta_{22} &= 2.505\times10^{-26} \text{ esu cm}^2 \\ \Theta_{33} &= -2.621\times10^{-26} \text{ esu cm}^2 \end{aligned} \tag{2.27}$$

The principal directions which diagonalize the quadrupole tensor here are just those which diagonalize the polarizability tensor, Eq. (2.25) above, so uniform notation has been used.

Dipole derivatives for the water molecule are also relevant to discussion of the dielectric response. Clough has determined the three first-order dipole derivatives from i.r. spectral intensities with the following results (Stillinger and David, 1978):

$$\begin{aligned} \left(\frac{\partial\mu}{\partial\theta}\right)_{r_1,r_2} &= -0.6830\times10^{-18} \text{ esu cm/rad} \\ \left(\frac{\partial\mu(||)}{\partial r_1}\right)_{\theta,r_2} &= 0.1568\times10^{-10} \text{ esu} \\ \left(\frac{\partial\mu(\perp)}{\partial r_1}\right)_{\theta,r_2} &= 0.7021\times10^{-10} \text{ esu} \end{aligned} \tag{2.28}$$

In these expressions r_1 and r_2 stand for the OH bond lengths, and θ stands for the bond angle. The dipole moment remains parallel to the molecular symmetry axis when only θ varies from the mechanical equilibrium point. But stretching a single bond destroys the C_{2v} molecular symmetry and causes the dipole to rotate as well as to change length. The latter two quantities in Eqs. (2.28) respectively give the variations

of the moment parallel to, and perpendicular to, the initial symmetry axis.

It is significant that the intramolecular charge rearrangement specified by Eqs. is substantially less (for both bend and stretch deformations) than would be expected if the effective atom charges 0.3289e and -0.6578e mentioned above were to move with the respective nuclei. Evidently the electron cloud undergoes a more complex adjustment as the nuclei move. The first of Eqs. (2.28) even has opposite sign to that of the naive atom-charge picture.

III. GENERAL THEORY

A. Molecular Interactions

The structure and properties of the condensed phases of water derive from the molecular interactions present. The nature of these interactions controls the form that the general statistical mechanical theory must take in order to describe dielectric phenomena. Therefore we begin this Section with a brief review of the nature of water molecule interactions.

In any collection of N water molecules, the nuclear geometry of molecule i ($1 \leq i \leq N$) can be denoted by a nine-component vector $\mathbf{X}_i$. Each such vector specifies not only the spatial position and orientation of the molecule, but its vibrational deformation as well. The general interaction for molecules described by $\mathbf{X}_1 \cdots \mathbf{X}_N$ (always assumed here to be in their electronic ground states) will be denoted by a potential energy function $V_N(\mathbf{X}_1 \cdots \mathbf{X}_N)$. It is useful to resolve V_N into components that are uniquely associated with single molecules ($V^{(1)}$), pairs of molecules ($V^{(2)}$), triplets of molecules ($V^{(3)}$), etc.

$$V_N(\mathbf{X}_1 \cdots \mathbf{X}_N) = \sum_{n=1}^{N} \sum_{i_1<\cdots<i_n=1}^{N} V^{(n)}(\mathbf{X}_{i_1} \cdots \mathbf{X}_{i_n}) \,. \tag{3.1}$$

the $V^{(n)}$ may be obtained from the V_N by successive reversion of the expressions (3.1)

for N=1,2,3... . The resulting expressions in leading order are the following:

$$\begin{aligned}
V^{(1)}(\mathbf{X}_1) &= V_1(\mathbf{X}_1) \,, \\
V^{(2)}(\mathbf{X}_1,\mathbf{X}_2) &= V_2(\mathbf{X}_1,\mathbf{X}_2) - V^{(1)}(\mathbf{X}_1) - V^{(1)}(\mathbf{X}_1) \,, \\
V^{(3)}(\mathbf{X}_1,\mathbf{X}_2,\mathbf{X}_3) &= V_3(\mathbf{X}_1,\mathbf{X}_2,\mathbf{X}_3) - V^{(1)}(\mathbf{X}_1) - V^{(1)}(\mathbf{X}_2) \\
&\quad - V^{(1)}(\mathbf{X}_3) - V^{(2)}(\mathbf{X}_1,\mathbf{X}_2) - V^{(2)}(\mathbf{X}_1,\mathbf{X}_3) \\
&\quad - V^{(2)}(\mathbf{X}_2,\mathbf{X}_3) \,.
\end{aligned} \tag{3.2}$$

Succeeding orders follow the same pattern; $V^{(n)}$ is the result of subtracting from V_n all possible $V^{(j)}$ for each proper subset of the n molecules.

By construction each $V^{(n)}$ for $n>1$ will vanish unless all n molecules are clustered together. So far as the single-molecule function is concerned it is convenient to choose the energy origin in such a way that $V^{(1)}$ vanishes when the three nuclei comprised by the molecule are at the mechanical equilibrium point.

The resolution of the total system potential V_N into inherent one, two, three,... molecule contributions is for water an arrangement in descending strength of interaction. The strongest forces present are intramolecular forces, which establish and maintain bond lengths and angles. $V^{(1)}$ contains this chemical bonding information, along with the specification of molecular deformation force fields which determine the three normal modes of vibration for the water molecule. The molecular pair potential $V^{(2)}$ by contrast is considerably weaker; nevertheless it is perhaps the most important of the interactions since it creates the intermolecular structure of the condensed phases. $V^{(3)}$ acts as a minor (but not entirely negligible) modulation effect on phase structure and properties, while $V^{(4)}, V^{(5)}$,... are thought to be generally insignificant.

The single most important feature conveyed by $V^{(2)}$ is the propensity for two water molecules to form a linear hydrogen bond. The geometry of the minimum-energy dimer (*i.e.* the absolute minimum for V_2) is indicated in Figure 1, and represents the

consensus of both experimental (Dyke, Mack, and Muenter, 1977) and theoretical (Stillinger, 1975) studies. The participating monomers are essentially unchanged from their free-molecule forms (due to the weakness of $V^{(2)}$ compared to the $V^{(1)}$'s). One molecule, the "proton donor", points an OH bond toward the oxygen atom of the other molecule, the "proton acceptor". The three pendant protons not directly involved in the hydrogen bond are located well off the OH···O bond axis. This optimal dimer has a plane of symmetry containing the proton donor, and the twofold axis of the acceptor molecule. Owing to the possibility of proton permutations, there are eight equivalent such dimer structures. The distance between the oxygens in this linear hydrogen bonding configuration is 2.98 ± 0.01Å. The strength of the bond is thought to be

$$V^{(2)}(\text{optimal}) \cong -5.0 \text{ kcal/mole} \quad . \tag{3.3}$$

While maintaining the linear hydrogen bond as shown in Figure 1, it costs relatively little energy to rotate the participating monomers through modest angles. This is true provided the proton acceptor molecule is not rotated so far as to bring one or

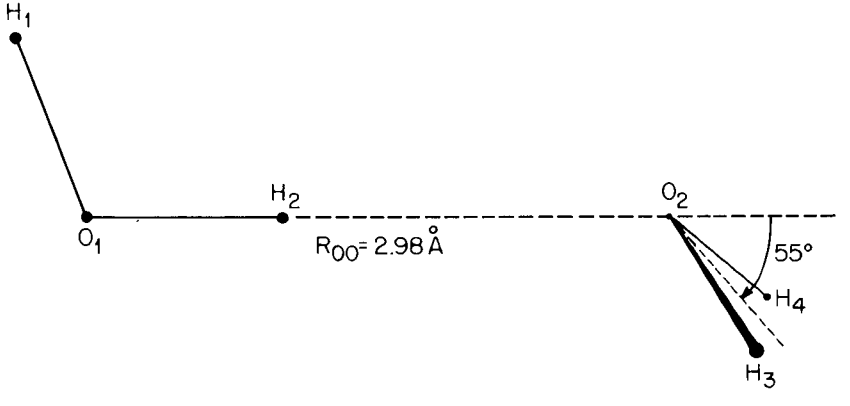

Figure 1. Structure of the minimum energy water dimer.

both of its pendant protons close to the given hydrogen bond. This angular flexibility permits hydrogen-bonded pairs in condensed phases to exist in a variety of relative geometries, and in particular permits any molecule to participate simultaneously in several hydrogen bonds both as donor and as acceptor. The natural mode of hydrogen-bond coordination is illustrated in ice [see Section V below] where each water molecule engages in exactly four tetrahedrally disposed hydrogen bonds.

As the distance between the oxygen atoms increases from the optimal 2.98Å, $V^{(2)}$ necessarily increases toward zero. At very large separations between the monomers $V^{(2)}$ reduces in form to that expected for point dipoles equal in magnitude to those of isolated molecules, Eq. (2.23). The minimum of this dipole-dipole interaction form, with respect to orientation angles, is achieved not in the hydrogen-bond configuration shown in Figure 1 but in a parallel-dipole arrangement which has different symmetry. It is known (Stillinger and Lemberg, 1975) that a critical intermediate distance exists at which $V^{(2)}$ manifests a sudden change between these two symmetries.

At small separation between the oxygen atoms (less than about 2.5Å) $V^{(2)}$ will be invariably positive for all relative molecular orientations. This reflects increasing overlap of the electron clouds of the two molecules which, on account of the exclusion principle, is energetically costly.

Figure 2 illustrates a water molecule surrounded by its natural complement of four hydrogen-bonded nearest neighbors. This is typical of the local geometry in the interior of ices Ih and Ic and in clathrate hydrates (Jeffrey, 1969). With some deformation of bond lengths and angles permitted it is also a frequently occurring arrangement in liquid water. Three distinct types of hydrogen-bonded trimers appear in this five-molecule complex, and $V^{(3)}$ depends significantly on which of the three is involved. The first is the "double donor" trimer, represented by ACE in Figure 2, with the central molecule A donating protons simultaneously to the two neighbors C and E. The

second is the "double acceptor" trimer, illustrated by ABD in Figure 2, in which the central molecule simultaneously accepts protons from its two neighbors. The third is the "sequential" trimer with the central molecule acting both as donor and as acceptor; BAC, BAD, DAC, and DAE are all of this last type.

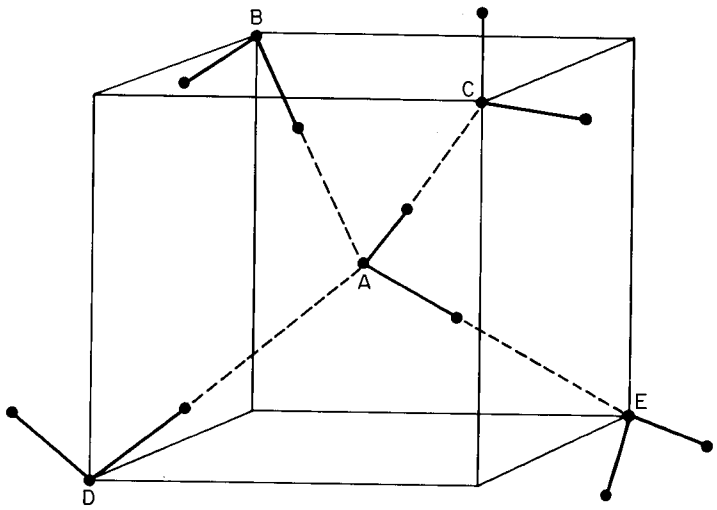

Figure 2. Natural fourfold coordination geometry for water molecules in condensed phases.

At present our only source of quantitative knowledge concerning $V^{(3)}$ has been quantum mechanical computation. All-electron *ab initio* calculations have been carried out for configurations of the sort illustrated in Figure 2 by Hankins, Moskowitz, and Stillinger (1970, 1973), by Del Bene and Pople (1973) and by Lentz and Scheraga (1973). These studies show that $V^{(3)}$ depends sensitively upon the pattern of hydrogen bonds present, but not very much on the position of pendant (nonbonded) hydrogens. At distances relevant to ice and to liquid water, the magnitudes are roughly the following:

$$\begin{aligned} V^{(3)} &\cong 1.2\text{kcal/mole (double donor)}, \\ &\cong 0.8\text{kcal/mole (double acceptor)} \\ &\cong -0.8\text{kcal/mole (sequential)} . \end{aligned} \tag{3.4}$$

These each appear to be monotonic with respect to mutual hydrogen bond length.

In any hydrogen bond network which has ubiquitous fourfold coordination as shown in Figure 2 there will be precisely six hydrogen-bonded trimers per molecule, in the ratios 1:1:4 for double donor, double acceptor, and sequential types (Hankins, Moskowitz, and Stillinger, 1970). The appropriate weighted average of $V^{(3)}$'s therefore is negative, and increasing in magnitude with decreasing distance. The net result is that three-body forces tend to increase overall binding energy in water molecule networks, and to decrease bond lengths. In respect to the latter it is useful to compare the isolated dimer bond length (2.98Å) with the nearest neighbor distance in ice at 0°K (2.74Å).

For trimers that are not connected by at least two well-formed hydrogen bonds, $V^{(3)}$ is probably not very large. If the three participating monomers are mutually well separated the resulting small $V^{(3)}$ could be well approximated by classical electrostatics, using the molecular permanent moments and polarizability tensors.

According to the work of Lentz and Scheraga (1973), $V^{(4)}$ tends to be an order of magnitude smaller even than $V^{(3)}$. By implication a similar decremental factor applies in going successively to $V^{(5)}$, $V^{(6)}$, etc.

Formation of a hydrogen bond between two water molecules causes rearrangement of charge within the pair. Quantum mechanical calculations indicate that the dimer at its most stable configuration has a significantly larger dipole moment than the vector sum of the monomer moments; Hankins, Moskowitz, and Stillinger (1970) found the enhancement to be 11 percent. The charge redistribution has been cited frequently as

an explanation of the differing signs displayed by $V^{(3)}$ for the distinct bonded trimer species (Del Bene and Pople, 1970).

It has already been remarked that water molecules in good approximation remain geometrically unperturbed by hydrogen bonding. However this is not exactly so. The covalent OH bond of a donated proton increases in length by about 0.005Å and the HOH angle of the acceptor molecule increases by about 0.5° (Stillinger, 1975) at the configuration of the optimal dimer (stationary nuclei). But more important than these small shifts is the reduction in stretching force constant for the bonding hydrogen by about 25 percent that is revealed by comparing vibrational frequencies for water vapor and for ice (Eisenberg and Kauzmann, 1969). This reduction in restoring force is probably accompanied by increasing anharmonicity of zero-point stretch motion, that would in turn produce an apparent stretch for the *mean* OH bond length. This effect, rather than the shift of the absolute potential minimum, is probably the dominating influence in measured stretches of OH covalent bond lengths in hydrogen-bonded solids (Olovsson and Jönsson, 1976).

The integrated intensity of OH stretch absorption in the infrared region experimentally undergoes an increase upon hydrogen bonding by approximately an order of magnitude (van Thiel, Becker, and Pimentel, 1957). Since these intensities are principally a measure of the square of the dipole derivative:

$$|\partial\mu/\partial r|^2 , \tag{3.5}$$

it is clear that one or both of the last two quantities in Eq. (2.28) has been strongly affected by formation of a linear hydrogen bond. The only reasonable interpretation of this phenomenon seems to be that the one-molecule solvation of a bonding hydrogen encourages it to act more and more as a bare proton as it departs from its parent oxygen. This interpretation is consistent with the fact that gas-phase dissociation produces uncharged radical fragments (H· and HO·) while condensed-phase dissociation

produces ions (H^+ and OH^-).

B. Formal Multipole Assignment

When two water molecules are engaged in a near-optimal hydrogen bond their electron clouds merge to some extent along the region of the OH···O axis. Hence it is not immediately obvious how one should assign multipole moments to the individual molecules involved. Obviously some scheme is necessary to partition space (and thus electronic charge) between the two. The potential ambiguity is aggravated in a large cluster where many hydrogen bonds can exist, and where shorter bonds produce a correspondingly greater electron cloud overlap.

We now construct a procedure which formally resolves all ambiguity. Its end result will be a set of nonoverlapping electron densities for each molecule. These densities yield precisely neutral molecules, and they can be used to compute multipole moments for each of the molecules.

The total electron charge present is -10Ne, where N is the number of molecules. For any given configuration of the nuclei there will be an electron charge density $\rho_e(\mathbf{r})$ that is a continuous and (except at the nuclei) differentiable function of position $\mathbf{r}$. Let us first divide space into ΩN convex non-overlapping regions each containing the *same* small amount of electron charge $-10e/\Omega$. If Ω is a large integer, most of the convex regions will be small; however a few at the periphery of the system may be large since ρ_e is small there. Our task then becomes that of assigning Ω regions to each H_2O triad of nuclei in an optimal fashion, and then allowing Ω to pass to infinity.

Let $1 \leq j \leq \Omega N$ index the regions, and let $1 \leq k \leq N$ index the nuclear triads. Then d_{jk} will be the distance between the centroid of the charge in region j, and the nearest of the three nuclei of triad k.

There will be exactly

$$(N\Omega)!/(\Omega!)^N \tag{3.6}$$

distinct ways to assign Ω regions to each triad. Most of these would be chemically absurd, since they would involve distances d_{jk} large on the molecular scale. Clearly it is desirable to eliminate these large-distance absurdities. This can be accomplished simply by minimizing the positive quantity

$$D(A) = \sum_{j=1}^{\Omega N} \sum_{k=1}^{N} d_{jk}^2(A) \tag{3.7}$$

with respect to assignments A. Except for zero-probability coincidences, we can take this D-minimizing A to be unique. The minimization has the global effect of clustering regions about triads.

We are still left with the necessity of passing to the infinite-Ω limit. This has the effect of shrinking to zero all region sizes (except for peripheral regions that become less and less important anyway). If this limit is achieved while retaining compact region shapes, it is clear that the union of regions for each nuclear triad will be bounded in that limit by piecewise smooth surfaces. Consequently each H_2O nuclear triad is surrounded by an electron distribution, containing precisely charge -10e, which does not overlap any other corresponding distribution. From these individual molecular charge distributions it is then a straightforward matter to calculate molecular multipole moments by the usual procedure.

One must keep in mind that the distinct molecular regions (as well as the electronic charge distributions they contain) will have shapes that generally depend on the presence or absence of externally applied fields.

C. Molecular Distribution Functions

While it is true in principle that nine coordinates are required to describe the nuclear configuration of a water molecule, a more compact description is warranted on

account of the stiffness of the molecule toward vibrational deformation. For much of the statistical mechanical theory of water it suffices to suppress the vibrational motions, and to treat the molecules as rigid rotors with C_{2v} symmetry. The original nine coordinates then shrink to six, which could be chosen for example as the oxygen nucleus position and three Euler angles for rotation about that position.

The possibility for such a reduction does not imply in any way that vibrational motions are unimportant. Indeed the coupling of vibrations to the other degrees of freedom as water molecules interact has important consequences for mean molecular moments and for binding energy in condensed phases. However it does mean that averaging properties over vibrational motions as a first step in the statistical mechanical theory is a simplifying and therefore useful tactic.

The process of projecting vibrational motions out of the theory causes the full nuclear potential $V_N(\mathbf{X}_1 \cdots \mathbf{X}_N)$, Eq. (3.1), to be replaced by

$$\bar{V}_N(\mathbf{x}_1 \cdots \mathbf{x}_N) = \sum_{n=1}^{N} \sum_{i_1 < \cdots < i_n = 1}^{N} \bar{V}^{(n)}(\mathbf{x}_{i_1} \cdots \mathbf{x}_{i_n}) \ , \tag{3.8}$$

where now each molecule j is described by a six-vector $\mathbf{x}_j$. The exact procedure by which V_N is replaced by $\bar{V}_N$ is described in Stillinger (1975). In most important respects the vibrationally averaged potentials $\bar{V}_N$ and $\bar{V}^{(n)}$ will be close to the corresponding unaveraged functions evaluated at the nuclear configurations for undeformed molecules (*i.e.* each molecule at its mechanical equilibrium point). However it is expected that the vibrational averaging will tend to enhance binding energies somewhat (Stillinger, 1975).

Once the strongly quantized vibrational motions have been removed from explicit consideration, it is reasonable to proceed with a purely classical statistical description. The overall configurational probability for N water molecules then can be taken to be the Boltzmann factor $\exp[-\beta(\bar{V}_N+U_N)]$ where β stands for $(k_BT)^{-1}$ as usual, and

where U_N stands for interaction with external fields (including electrical fields).

The full N-molecule probability is unnecessarily complicated for understanding properties of normal interest. Instead it usually suffices to consider configurational probability functions for small sets of particles, and this is certainly true for the present study of static dielectric behavior. Therefore we contract the full-system Boltzmann factor to a set of molecular distribution functions as follows (n=1,2,3...):

$$\rho^{(n)}(\mathbf{x}_1 \cdots \mathbf{x}_n) = \frac{N(N-1)...(N-n+1)\int d\mathbf{x}_{n+1} \cdots \int d\mathbf{x}_N \exp[-\beta(\overline{V}_N+U_N)]}{\int d\mathbf{x}_1 \cdots \int d\mathbf{x}_N \exp[-\beta(\overline{V}_N+U_N)]} \quad (3.9)$$

the integrals span the system volume V and the molecular rigid-body rotations for the indicated particles. The meaning of $\rho^{(n)}$ is simply the probability density in the space of sets of six-vectors $\mathbf{x}_1 \cdots \mathbf{x}_n$ for occurrence of the given n-molecule configuration.

The simplest of the molecular distribution functions is $\rho^{(1)}(\mathbf{x}_1)$. In the case of an isotropic liquid or vapor phase that is not perturbed by external fields (U_N=0) $\rho^{(1)}$ is independent of $\mathbf{x}_1$:

$$\rho^{(1)}(\mathbf{x}_1) \rightarrow N/(8\pi^2 V) \quad \text{(isotropic fluid)} . \quad (3.10)$$

Upon crystallization to form ice, long-range order sets in. If boundary conditions clamp the resulting crystal in a fixed spatial position $\rho^{(1)}(\mathbf{x}_1)$ will no longer be equal to the above constant value. Instead it will display periodic behavior with respect to translation, and it will manifest sets of preferred orientations at lattice sites and at interstitial positions respectively.

Upon subjecting the N-molecule system to an external electric field, $\rho^{(1)}$ changes to reflect the induced polarization **P**. It is one of our objectives in following Sections to calculate those changes.

The molecular pair distribution function $\rho^{(2)}$ generally plays a fundamental role in the statistical mechanics of condensed matter, and it has particular importance for the theory of static dielectric behavior. Several of its properties deserve to be mentioned at the outset. The first and most elementary of these is the contraction property which follows immediately from the definition (3.9),

$$\int d\mathbf{x}_2 \rho^{(2)}(\mathbf{x}_1,\mathbf{x}_2) = (N-1)\rho^{(1)}(\mathbf{x}_1) . \quad (3.11)$$

The second applies in the large-system limit for which large separation r_{12} between the two molecular centers can be achieved:

$$\rho^{(2)}(\mathbf{x}_1,\mathbf{x}_2) \rightarrow \rho^{(1)}(\mathbf{x}_1)\rho^{(1)}(\mathbf{x}_2) \quad (\text{large } r_{12}) \quad (3.12)$$

"Large r_{12}" in this context means "many molecular diameters". This asymptotic factorization states that pairs of widely separated molecules within a large system will be correlated only by long-range crystalline order (if it is present), or by macroscopic polarization.

On account of Eq. (3.12) it is useful to isolate small-distance deviations from the factoring limit in the "pair correlation function" $g^{(2)}$, defined by

$$\rho^{(2)}(\mathbf{x}_1,\mathbf{x}_2) = \rho^{(1)}(\mathbf{x}_1)\rho^{(1)}(\mathbf{x}_2)g^{(2)}(\mathbf{x}_1,\mathbf{x}_2) . \quad (3.13)$$

If the separation r_{12} between molecular centers is substantially smaller than the normal nearest neighbor distance, strong repulsive forces will be present which drive $g^{(2)}$ (and with it $\rho^{(2)}$) to zero. By contrast we expect the maximum value of $g^{(2)}$ to be achieved when $\mathbf{x}_1$ and $\mathbf{x}_2$ conform to the geometry of nearly optimal dimer hydrogen bonding, *i.e.*, to the minimum in $\overline{V}^{(2)}(\mathbf{x}_1,\mathbf{x}_2)$. Beyond the nearest-neighbor separation $g^{(2)}$ reflects a combination of direct interaction between the participating molecules as well as indirect medium effects due to the influence of surrounding molecules.

There are two measures of molecular orientational correlation that traditionally have entered discussion of polar dielectrics, which we will denote simply as G and g respectively. Both can be expressed in terms of the pair distribution function $\rho^{(2)}$ for the field-free system. Let $\mathbf{u}_j$ stand for a unit vector embedded in molecule j and point-

ing along its twofold symmetry axis. The vector sum of all such $\mathbf{u}_j$ defines

$$\mathbf{t} = \sum_{j=1}^{N} \mathbf{u}_j \ . \tag{3.14}$$

The mean square value of t averaged over all molecular positions and orientations in the canonical ensemble is easily shown to be the following:

$$\begin{aligned} <t^2> &= N+N(N-1)<\mathbf{u}_1\cdot\mathbf{u}_2> \\ &= N+\int d\mathbf{x}_1 \int d\mathbf{x}_2 (\mathbf{u}_1\cdot\mathbf{u}_2)\rho^{(2)}(\mathbf{x}_1,\mathbf{x}_2) \end{aligned} \tag{3.15}$$

In fact the $\rho^{(2)}$ integral in this last expression will be proportional to N in the large-system limit, so we write

$$<t^2> = NG, \tag{3.16}$$

where

$$G = 1+ \lim_{N,V\to\infty} N^{-1} \int_V d\mathbf{x}_1 \int_V d\mathbf{x}_2 (\mathbf{u}_1\cdot\mathbf{u}_2)\rho^{(2)}(\mathbf{x}_1,\mathbf{x}_2) \ . \tag{3.17}$$

The symbol "V" has been appended to this expression as an explicit reminder that the molecular positions are allowed to span the entire system volume. For totally uncorrelated molecular orientations G=1. The extent to which G deviates from 1 measures orientational correlation in the system, with G>1 indicating a tendency toward alignment of molecular symmetry axes. The alternative quantity g is defined by an expression that looks deceptively similar to Eq. (3.17):

$$g = 1 + \lim_{\omega\to\infty} \lim_{N,V\to\infty} (V/N\omega) \int_\omega d\mathbf{x}_1 \int_\omega d\mathbf{x}_2 (\mathbf{u}_1\cdot\mathbf{u}_2)\rho^{(2)}(\mathbf{x}_1,\mathbf{x}_2) \ . \tag{3.18}$$

In this case the positional integrations are restricted to a fixed subvolume ω within the system volume V, the latter is allowed to go to infinity (at constant density N/V), and *then finally* ω is itself allowed to become infinite. It is one of the intriguing subtleties of dielectric theory that G and g are *not* equivalent, the reasons for which should later become apparent.

The quantity g was originally introduced into dielectric theory by Kirkwood (1939), whereas Slater (1941) and Onsager and Dupuis (1960) are usually credited with having first emphasized the role of G.

In the case of isotropic fluids G and g can be simply expressed in terms of the pair correlation function $g^{(2)}$:

$$G = 1 + (\rho/8\pi^2) \lim_{N,V\to\infty} \int_V d\mathbf{x}_2 (\mathbf{u}_1\cdot\mathbf{u}_2) g^{(2)}(\mathbf{x}_1,\mathbf{x}_2) \ ; \tag{3.19}$$

$$g = 1 + (\rho/8\pi^2) \lim_{\omega\to\infty} \lim_{N,V\to\infty} \int_\omega d\mathbf{x}_2 (\mathbf{u}_1\cdot\mathbf{u}_2) g^{(2)}(\mathbf{x}_1,\mathbf{x}_2) \ , \tag{3.20}$$

where ρ=N/V is the molecular number density.

Because any given water molecule possesses a permanent dipole moment, that molecule acts as an electric field source to which the other nearby molecules respond. The average response of those surrounding molecules will be that of a polarization field with dipolar symmetry, at least at reasonably large distances on the molecular scale. It has been pointed out before (Stillinger, 1970) that this fact leads for fluids to an explicit form for $g^{(2)}(\mathbf{x}_1,\mathbf{x}_2) - 1$ at large r_{12}, provided a simplifying assumption is valid. This assumption is that the dipole moments of each molecule have negligible fluctuations about a mean magnitude $\bar{\mu}$, and are aligned along the molecular symmetry axes. Thereupon we have (in the infinite system limit):

$$g^{(2)}(\mathbf{x}_1,\mathbf{x}_2)-1 \sim \frac{9g(\epsilon_0-1)}{4\pi\rho(2\epsilon_0+1)} \mathbf{u}_1 \cdot \mathbf{T}_{12} \cdot \mathbf{u}_2 \ , \tag{3.21}$$

where $\mathbf{T}_{12}$ is the characteristic tensor for dipole-dipole interactions,

$$\mathbf{T}_{12} = \frac{1}{r_{12}^3} \left[1 - \frac{3\mathbf{r}_{12}\mathbf{r}_{12}}{r_{12}^2} \right] . \tag{3.22}$$

Although the Kirkwood correlation factor g appears in the asymptotic form (3.21), it is interesting to note that this limiting large-r_{12} dipolar term does *not* contribute anything to the defining integral for g in Eq. (3.20).

IV. LIQUID WATER

A. Local Order

Figure 2 has illustrated the local four-fold coordination via hydrogen bonding that holds the ice crystal together. Excepting the neighborhood of rare defects, this pattern obtains at every lattice position within the interior of an ice crystal and creates long-range order. It also creates the rigidity which ice exhibits.

Melting of the ice phase to produce liquid water fundamentally disrupts the order initially present. Long-range periodic order (measured by variations in $\rho^{(1)}(\mathbf{x})$ about its mean) disappears altogether, while short-range order (manifest in $g^{(2)}(\mathbf{x}_1, \mathbf{x}_2)$ over the first few molecular diameters is sharply reduced. This sudden introduction of disorder at the melting point is quantitatively revealed by the measured entropy of fusion,

$$\Delta S/Nk_B = 2.646 \ . \tag{4.1}$$

For the purpose of qualitatively guiding one's intuition about the melting transition it is useful to think in terms of an increase in the configurational freedom per molecule attendant upon melting. The appropriate factor is supplied by the exponential of quantity (4.1):

$$\exp(\Delta S/Nk_B) = 14.10 \ . \tag{4.2}$$

The most appropriate view of liquid water is that it consists of a random, defective, space-filling network (Stillinger, 1977). On the basis of computer simulation studies (Rahman and Stillinger, 1973) it is believed that the invariant ice-like pattern of four hydrogen bonds to each molecule is replaced by a broad distribution of 0 to 5 bonds, with a mean around 2.5 . Furthermore the bonds that are present form polygonal closures with no preference for even versus odd numbers of bonds; by contrast the crystal structures of hexagonal and cubic ice exhibit polygonal closures with only even numbers (6,8,10,12,...) of sides. It has also been established (Geiger, Stillinger, and Rahman, 1979) that with any reasonable definition of "hydrogen bond" liquid water at ordinary temperatures is above the critical percolation threshold, *i.e.* the liquid essentially consists of a single macroscopic cluster of molecules connected by hydrogen bonds. Consequently it is inappropriate to view liquid water as consisting of disconnected microscopic clusters of bonded molecules floating about in a medium of unbonded molecules, though in fact this picture has enjoyed a considerable historical prominence (Kavanau, 1964).

Evidently the local molecular order surrounding any chosen water molecule in the liquid is quite variable. The variations include the number of hydrogen bonds terminating at that molecule, their lengths and directions, and the possible presence of close but unbonded neighbors. It was remarked above (Sect. III. A) that hydrogen bonding affects the electrical properties of the participating monomers, in particular their dipole moments. Consequently any credible molecular theory of the dielectric constant in liquid water ought to include an account of the fluctuating local order.

B. "Kirkwood" Dielectric Formula

Our next objective is to deduce an expression for the static dielectric constant ϵ_0 in terms of molecular parameters that characterize the liquid. The resulting formula, Eq. (4.27) below, will be a modification and generalization of one originally derived by Kirkwood (1939) for polar fluids. Our derivation parallels those of Harris and Alder (1953) and of Buckingham (1956) but with some changes motivated by the present more complete understanding of molecular interactions in water.

For the sake of convenience it will be supposed that suitable boundaries are present to confine the liquid sample (N molecules) to a spherical shape (volume V).

These boundary conditions serve *only* to maintain the geometric shape of the macroscopic sample, and have no further implication for the electrical behavior to be investigated.

Now let this spherical sample be placed within a region of space which, when originally empty, possessed a uniform electric field directed along the z axis:

$$\mathbf{E}_0 = E_0 \, \mathbf{u}_z \ . \tag{4.3}$$

We shall suppose that this field is sufficiently weak that it creates linear response only. Macroscopic electrostatics applied to our spherical homogeneous dielectric states that the mean electrical field $\mathbf{E}$ within the system is parallel to $\mathbf{E}_0$ and has the magnitude

$$\mathbf{E} = \left(\frac{3}{\epsilon_0 + 2} \right) \mathbf{E}_0 \ . \tag{4.4}$$

From this we can infer the polarization $\mathbf{P}$ via the fundamental relation Eq. (2.2):

$$\left(\frac{\epsilon_0 - 1}{\epsilon_0 + 2} \right) \mathbf{E}_0 = \left(\frac{4\pi}{3} \right) \mathbf{P} \ . \tag{4.5}$$

Statistical mechanical theory also supplies an expression for $\mathbf{P}$, namely

$$\mathbf{P} = <\mathbf{M}(\mathbf{x}_1 \cdots \mathbf{x}_N, \mathbf{E}_0)>/V \ , \tag{4.6}$$

where $\mathbf{M}$ is the total moment of the system when the N molecules have fixed positions and orientations $\mathbf{x}_1 \cdots \mathbf{x}_N$, and when the external homogeneous field is $\mathbf{E}_0$. The average indicated in Eq. (4.6) involves a canonical distribution with this external field present. Consequently we have

$$\frac{\epsilon_0 - 1}{\epsilon_0 + 2} = \frac{4\pi \int d\mathbf{x}_1 \cdots \int d\mathbf{x}_N \, (\mathbf{M} \cdot \mathbf{u}_z) \exp[-\beta(\bar{V}_N + U_N)]}{3V E_0 \int d\mathbf{x}_1 \cdots \int d\mathbf{x}_N \exp[-\beta(\bar{V}_N + U_N)]} \tag{4.7}$$

As before $\bar{V}_N$ stands for the molecular interaction potential within the system, and is independent of $\mathbf{E}_0$; U_N is the interaction of the collection of molecules with $\mathbf{E}_0$.

Since interest is confined to linear response it will suffice to retain only terms through linear order in $\mathbf{E}_0$ in the expansions of U_N and of $\mathbf{M}$. The former has the following form:

$$U_N(\mathbf{x}_1 \cdots \mathbf{x}_N, \mathbf{E}_0) = -\mathbf{M}(\mathbf{x}_1 \cdots \mathbf{x}_N, 0) \cdot \mathbf{E}_0 + 0(E_0^2) \ , \tag{4.8}$$

which to the requisite order involves only the spontaneous moment of the system in the given configuration. For the latter we can quite generally write:

$$\mathbf{M}(\mathbf{x}_1 \cdots \mathbf{x}_N, \mathbf{E}_0) = \mathbf{M}(\mathbf{x}_1 \cdots \mathbf{x}_N, 0) + \mathbf{M}_1(\mathbf{x}_1 \cdots \mathbf{x}_N) \cdot \mathbf{E}_0 + 0(E_0^2) \tag{4.9}$$

where again the spontaneous moment appears in leading order, and where the tensor $\mathbf{M}_1$ is defined:

$$\mathbf{M}_1 = \left(\frac{\partial \mathbf{M}}{\partial \mathbf{E}_0} \right)_{\mathbf{E}_0 = 0} \ . \tag{4.10}$$

Although $\mathbf{M}_1$ in principal is a complicated quantity that is difficult to compute in general, it should suffice for the task in hand to replace it by an average value that is suggested by macroscopic considerations. After all $\mathbf{M}_1$ represents the *extra* moment linearly induced in the system by $\mathbf{E}_0$ when the molecular configurations $\mathbf{x}_1 \cdots \mathbf{x}_N$ are fixed. For virtually all configurations this extra moment will be nearly parallel to $\mathbf{E}_0$. It is furthermore determined by electronic polarization and by deformations in vibrational degrees of freedom that result as $\mathbf{E}_0$ shifts mechanical equilibrium points. These considerations suggest that we write $\mathbf{M}_1$ in terms of the high frequency dielectric constant ϵ_h which refers to a regime in frequency too high for the orientations to respond at all, but low enough so that vibrational shifts can so respond. Appealing

once again to the electrostatic solution for the sphere we thus have

$$\mathbf{M}_1 \to \frac{3V}{4\pi}\left(\frac{\epsilon_h - 1}{\epsilon_h + 2}\right)\mathbf{E}_0 1 \quad , \tag{4.11}$$

and so Eq. (4.9) becomes

$$\mathbf{M}(\mathbf{x}_1 \cdots \mathbf{x}_N, \mathbf{E}_0) = \mathbf{M}(\mathbf{x}_1 \cdots \mathbf{x}_N, 0) + \frac{3V}{4\pi}\left(\frac{\epsilon_h - 1}{\epsilon_h + 2}\right)\mathbf{E}_0 + 0(E_0^2) \quad . \tag{4.12}$$

After inserting expressions (4.8) and (4.12) into Eq. (4.7), and discarding all but the leading-order terms in E_0, we obtain

$$\frac{\epsilon_0 - 1}{\epsilon_0 + 2} = \frac{\epsilon_h - 1}{\epsilon_h + 2} + \frac{4\pi\beta}{3V} <[\mathbf{M}(\mathbf{x}_1 \cdots \mathbf{x}_N, 0) \cdot \mathbf{u}_z]^2>_{E_0=0} \quad . \tag{4.13}$$

As indicated by the subscript E_0=0 the average appearing here refers to the field-free ensemble. On account of isotropy of the liquid sample the last equation can equally well be written

$$\frac{\epsilon_0 - 1}{\epsilon_0 + 2} = \frac{\epsilon_h - 1}{\epsilon_h + 2} + \frac{4\pi\beta}{9V} <[\mathbf{M}(\mathbf{x}_1 \cdots \mathbf{x}_N, 0)]^2>_{E_0=0} \quad . \tag{4.14}$$

We see from this intermediate result that contribution of orientational motions to ϵ_0 is contained in the mean-square fluctuations in the system moment.

The next step is to express the average in Eq. (4.14) in terms of relatively simple molecular distribution functions. First recall that the procedure of Sec. III. B above permits us to assign moments uniquely to each molecule, so the total system moment **M** is simply the sum of those individual moments:

$$\mathbf{M}(\mathbf{x}_1 \cdots \mathbf{x}_N, 0) = \sum_{j=1}^{N} \boldsymbol{\mu}_j (\mathbf{x}_1 \cdots \mathbf{x}_N, 0) \quad . \tag{4.15}$$

The notation here stresses the important fact that on account of interactions each of the molecular moments depends in principle upon the entire set of configurational coordinates $\mathbf{x}_1 \cdots \mathbf{x}_N$. Inserting Eq. (4.15) into Eq. (4.14) we obtain

$$\frac{\epsilon_0 - 1}{\epsilon_0 + 2} = \frac{\epsilon_h - 1}{\epsilon_h + 2} + \left(\frac{4\pi\rho\beta}{9}\right) <\boldsymbol{\mu}_1 \cdot \mathbf{M}> \quad , \tag{4.16}$$

where ρ stands for the number density N/V. [Here and in the following we assume the averages all refer to $E_0 = 0$, so having that as a subscript is unnecessary.] Of course we can also write

$$<\boldsymbol{\mu}_1 \cdot \mathbf{M}> = <\mu_1^2> + (N-1)<\boldsymbol{\mu}_1 \cdot \boldsymbol{\mu}_2> \quad . \tag{4.17}$$

Kirkwood's perceptive contribution to the theory of polar dielectrics was to identify two distinct contributions to the average appearing in Eq. (4.16). The first is concentrated in the immediate neighborhood of molecule 1 and arises from a local moment $\mathbf{m}_1^*$ due to molecule 1 and its immediate neighbors whose rotations are hindered by interaction with 1. The second is a more subtle contribution that arises from the electrostatic boundary conditions at the spherical surface of the sample. The local moment $\mathbf{m}_1^*$ induces in the sample a polarization field containing throughout **V** a uniform component antiparallel to $\mathbf{m}_1^*$. This uniform component is very weak for a large system volume **V**; it is in fact proportional to $\mathbf{V}^{-1}$. But upon integrating this weak polarization over **V** to find the corresponding contribution to the total moment **M**, it is clear that a result independent of **V** emerges. We refer the reader to Kirkwood (1939) for the detailed electrostatic calculation of this effect. The net result is that in Eq. (4.16) we can set

$$\mathbf{M} = \frac{9\epsilon_0}{(2\epsilon_0+1)(\epsilon_0+2)}\,\mathbf{m}_1^* \quad . \tag{4.18}$$

As a consequence,

$$\frac{\epsilon_0 - 1}{\epsilon_0 + 2} = \frac{\epsilon_h - 1}{\epsilon_h + 2} + \frac{4\pi\rho\beta\epsilon_0}{(2\epsilon_0+1)(\epsilon_0+2)} <\boldsymbol{\mu}_1 \cdot \mathbf{m}_1^*> \ , \tag{4.19}$$

which thus expresses ϵ_0 in terms of strictly local fluctuating moments.

The moment $\boldsymbol{\mu}_1$ fluctuates on account of variations from instant to instant in the extent to which molecule 1 interacts with its neighbors. In particular the number and strength of the hydrogen bonds it makes to its immediate neighbors is relevant, with each hydrogen bond tending to increase the magnitude of $\boldsymbol{\mu}_1$ above the isolated molecule value. The more complicated quantity $\mathbf{m}_1^*$ fluctuates not only due to $\boldsymbol{\mu}_1$ variations, but due as well to changing patterns of partially aligned neighbors arranged around molecule 1. If it were the case that the dipole moments of all molecules could be treated as independently fluctuating, then it is easy to see that

$$<\boldsymbol{\mu}_1 \cdot \mathbf{m}_1^*> = <\boldsymbol{\mu}_1^2> g \ , \tag{4.20}$$

where g is the Kirkwood orientational correlation factor defined earlier in Eq. (3.18). The implication would be

$$\frac{\epsilon_0 - 1}{\epsilon_0 + 2} = \frac{\epsilon_h - 1}{\epsilon_h + 2} + \frac{4\pi\rho\beta g\epsilon_0}{(2\epsilon_0+1)(\epsilon_0+2)} <\boldsymbol{\mu}_1^2> \ . \tag{4.21}$$

The fact remains that correlated moment fluctuations are likely to have a significant influence on ϵ_0 for liquid water. As any given hydrogen bond forms and breaks in the liquid *two* molecules which are neighbors are involved. Consequently we expect a positive correlation for the magnitudes of their fluctuating moments (both moments enhanced by an intact bond, both diminished when it breaks). Therefore it is necessary to replace the naive Eq. (4.21) by a suitably modified alternative.

Define the following quantity:

$$s(\mathbf{x}_1^{(0)}, \mathbf{x}_2^{(0)}) = <(\boldsymbol{\mu}_1 \cdot \boldsymbol{\mu}_2)\ \delta\ (\mathbf{x}_1 - \mathbf{x}_1^{(0)})\ \delta\ (\mathbf{x}_2 - \mathbf{x}_2^{(0)})> \ , \tag{4.22}$$

i.e. the mean value of the scalar product of $\boldsymbol{\mu}_1$ and $\boldsymbol{\mu}_2$ subject to the respective molecules having configurational coordinates $\mathbf{x}_1^{(0)}$ and $\mathbf{x}_2^{(0)}$. In terms of this function it is clear that

$$<\boldsymbol{\mu}_1 \cdot \mathbf{m}_1^*> = <\boldsymbol{\mu}_1^2> + \lim_{\omega\to\infty} \lim_{V\to\infty} (\rho/8\pi^2)$$

$$\times \int_\omega d\mathbf{x}_2\, s(\mathbf{x}_1, \mathbf{x}_2)\, g^{(2)}(\mathbf{x}_1, \mathbf{x}_2) \tag{4.23}$$

where ω, a fractionally small subregion of V, is centered around molecule 1. It is useful to write

$$<\boldsymbol{\mu}_1 \cdot \mathbf{m}_1^*> = <\boldsymbol{\mu}_1^2>[1 + (g-1)\phi] \tag{4.24}$$

where ϕ=1 for independently fluctuating molecular moments, but where more generally

$$\phi = \lim_{\omega\to\infty} \lim_{V\to\infty} \frac{\int_\omega d\mathbf{x}_2\, s(\mathbf{x}_1, \mathbf{x}_2)\, g^{(2)}(\mathbf{x}_1, \mathbf{x}_2)}{<\boldsymbol{\mu}_1^2> \int_\omega d\mathbf{x}_2\, \boldsymbol{\mu}_1 \cdot \boldsymbol{\mu}_2\, g^{(2)}(\mathbf{x}_1, \mathbf{x}_2)} \ . \tag{4.25}$$

From what has been said repeatedly about molecular interactions in liquid water we certainly expect to have

$$\phi \neq 1 \ , \tag{4.26}$$

though the magnitude of this quantity is not obvious.

By combining Eqs. (4.19) and (4.24) we obtain

$$\frac{\epsilon_0 - 1}{\epsilon_0 + 2} = \frac{\epsilon_h - 1}{\epsilon_h + 2} + \frac{4\pi\rho\beta\epsilon_0}{(2\epsilon_0+1)(\epsilon_0+2)} [1 + (g-1)\ \phi] <\boldsymbol{\mu}_1^2> \ . \tag{4.27}$$

This is the desired modification of Eq. (4.19) to account for correlated moment fluctuations. It can be viewed as an updated version of the Kirkwood dielectric formula (Kirkwood, 1939).

C. Numerical Estimates

At any given temperature and pressure (*i.e.* density) the fundamental formula (4.27) for ϵ_0 contains four parameters: ϵ_h, g, ϕ, and $<\mu_1^2>$. The first of these is a macroscopic property directly accessible from experiment. The other three are microscopic properties for which no direct measurement techniques are available.

It was remarked above that ϵ_h should be the dielectric constant for a frequency range above which vibrational motions occur, but below which rotational degrees of freedom are evident. The lower of the two main vibrational bands observed spectroscopically in water is centered around 1650 cm^{-1}, while librations (the highest frequency rotational motions) produce a band centered near 700 cm^{-1} (Eisenberg and Kauzmann, 1969). Consequently ϵ_h should refer to the frequency region around 1200 cm^{-1}. Measurements of the real and imaginary refractive indices are available in this region (Querry, Curnutte, and Williams, 1969) from which we conclude

$$\epsilon_h = 1.64 \qquad (24°C) \ . \tag{4.28}$$

There is no reason to believe this would be strongly temperature-dependent.

Several estimates of the Kirkwood orientational factor g in water have been published. The first was due to Kirkwood himself (Kirkwood, 1939). The point of view taken for that estimate was that each molecule was surrounded by a rigorously tetrahedral grouping of four nearest neighbors (as in ice, see Fig. 2), but that each of these neighbors was free to rotate about the hydrogen bond direction determined by lone-pair electron orbitals. No contributions to g from molecules beyond this first

coordination shell were considered. In a crude sense this is consistent with the fact that only short-range order is present in liquids. Kirkwood's result was

$$g \cong 2.64 \ , \tag{4.29}$$

and is manifestly temperature and density independent.

Pople has devised a more satisfactory method of calculating g (Pople, 1951). Although his model continues to assume each molecule is hydrogen bonded to exactly four nearest neighbors, thermally activated bending of those bonds (as well as rotation) is permitted. Furthermore local order through bendable hydrogen bonds is considered up through a third coordination shell. Pople obtains the following results:

$$\begin{aligned} g &= 2.60 \quad (0°C) \\ &\ \ 2.55 \quad (25°C) \\ &\ \ 2.49 \quad (62°C) \\ &\ \ 2.46 \quad (83°C) \end{aligned} \tag{4.30}$$

The decline of orientational correlation with increasing temperature seems at least intuitively reasonable. The number shown for g at 0°C is composed of the contributions 1.00, 1.20, 0.33, and 0.07 corresponding to the central molecule itself, the first shell of neighbors, the second shell, and the third shell. The calculation thus demonstrates its own internal consistency in neglect of neighbors beyond the third shell.

Computer simulation of liquid water offers a way to avoid the assumption of invariant fourfold coordination. At the same time a new set of difficulties arise, namely that the collections of molecules usually considered are very small (usually N is in the range 10^2 to 10^3), and the interactions employed involve simplifications (pairwise additivity, most significantly). Nevertheless it is worthwhile noting that g has been estimated on the basis of at least one molecular dynamics study (Stillinger and

Rahman, 1974). This study employed 216 molecules, periodic boundary conditions, and the so-called "ST2" pair potential. g was not computed directly (the system was too small), but was inferred from the observed values of G [defined in Eq. (3.17)]. The following values were reported for the liquid at $1\,g/cm^3$:

$$\begin{aligned} g = 3.66 \quad & (-3^\circ C) \\ 2.88 \quad & (10^\circ C) \\ 2.68 \quad & (41^\circ C) \\ 2.52 \quad & (118^\circ C) \ . \end{aligned} \tag{4.31}$$

Since there are some indications that this model for water possesses local structure that is a bit too well developed, it may be that these numbers in Eq. (4.31) are larger than the correct values. No doubt future simulations will yield more precise and reliable values for g.

Just as for g these are several calculations in print for the mean dipole moment in liquid water. On account of the foregoing general theory culminating in Eq. (3.27), we take the "mean moment" to stand for the quantity $<\mu^2>^{1/2}$. Using classical electrostatics and Pople's model for local order in water (Pople, 1951), Eisenberg and Kauzmann (1969) conclude that

$$\begin{aligned} <\mu^2>^{1/2} = 2.45 \text{ D} \quad & (0^\circ C) \\ 2.37 \text{ D} \quad & (83^\circ C) \end{aligned} \tag{4.32}$$

This should be compared with the vapor phase moment 1.855 D mentioned earlier [Eq. (2.23)].

An independent estimate can be obtained, perhaps reasonably, by interpolating between the vapor phase value just mentioned, and the mean moment for ice near its melting point. Wörz and Cole (1969) have calculated the latter to be

$$<\mu^2>^{1/2} = 2.73 \text{ D} \ , \tag{4.33}$$

a result that has Onsager's subsequent endorsement (Onsager, 1973). Since the dipole enhancements in condensed phases are due to interactions it seems sensible to suppose that those enhancements are directly proportional to binding energies of those phases. These binding energies are thermodynamically available as energies of evaporation. On this basis one readily calculates for the liquid

$$<\mu^2>^{1/2} = 2.62 \text{ D} \quad (0^\circ C) \ . \tag{4.34}$$

This interpolative result presumably includes the specific quantum-mechanical effects of hydrogen bonding on electronic structure and on the average nuclear geometry of the water molecule embedded in the liquid. By contrast the Eisenberg-Kauzmann results shown in Eq. (4.32) utilize classical electrostatics with inclusion only of electronic polarizability. For this reason Eq. (4.34) may give the more reliable estimate.

Unlike the cases of g and of $<\mu^2>^{1/2}$, no estimates of the dipole fluctuation correlation parameter ϕ have been published. Indeed even qualitative mention of the effects embodied in this quantity seem not to have intruded into previous discussions of the theory of polar dielectrics. For present purposes we will be content to arrive at a rough value of ϕ by inverting Eq. (4.27):

$$\phi = \frac{1}{g-1}\left\{\frac{(2\epsilon_0+1)(\epsilon_0+2)}{4\pi\rho\beta\epsilon_0<\mu^2>}\left[\frac{\epsilon_0-1}{\epsilon_0+2}-\frac{\epsilon_h-1}{\epsilon_h+2}\right]-1\right\} \ , \tag{4.35}$$

and then inserting appropriate values into the right hand side. In view of the preceding discussion we assume the following values apply for the liquid at 0°C:

$$\epsilon_0 = 87.74$$

$$\epsilon_h = 1.64$$

$$\rho = 3.343 \times 10^{22}\ \mathrm{cm}^{-3}$$

$$g = 2.60$$

$$<\mu^2> = 6.86\ \mathrm{D}^2 \ . \qquad (4.36)$$

When these are inserted in Eq. (4.35) the result is

$$\phi = 0.54 \quad (0°\mathrm{C}) \ . \qquad (4.37)$$

It needs to be stressed that this result is sensitive mostly to the value assumed for the mean square liquid-phase dipole moment. As this latter quantity decreases, ϕ increases. Holding the other parameters at the values shown in Eq. (4.36), ϕ passes through 1 when

$$<\mu^2>^{1/2} = 2.22\ \mathrm{D} \ . \qquad (4.38)$$

This seems rather smaller than can comfortably be assumed for the liquid at 0°C. Consequently ϕ probably is actually less than 1.

The *magnitudes* of neighboring dipole moments in the liquid are expected to exhibit positive correlation as hydrogen bond linkages between the molecules form and break. That ϕ should be less than unity indicates that the defining expression (4.25) receives substantial contributions from pairs of molecules for which

$$\boldsymbol{\mu}_1 \cdot \boldsymbol{\mu}_2 < 0 \ . \qquad (4.39)$$

This situation is possible for directly hydrogen-bonded molecules if (see Figure 1) the angle made by the acceptor molecule axis is sufficiently large with respect to the

hydrogen bond axis. It is also easily possible for a pair of second neighbors along a chain of hydrogen bonds as illustrated by Figure 3. This latter arrangement is reasonable in view of the apparent existence of many closed hydrogen bond polygons in the liquid (Rahman and Stillinger, 1973).

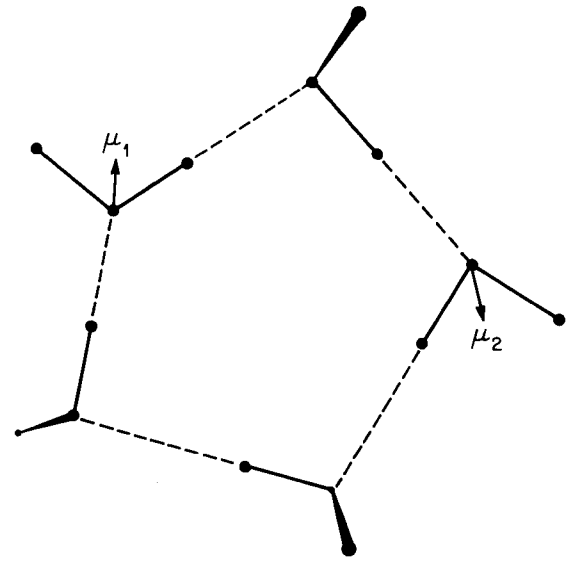

Figure 3. Tendency toward dipole antiparallelism ($\boldsymbol{\mu}_1 \cdot \boldsymbol{\mu}_2 < 0$) for second neighbors along a chain of hydrogen bonds.

It is an unfortunate fact that we have only crude estimates for the important quantities $<\mu^2>^{1/2}$, g, and ϕ in liquid water. Obviously some concentrated theoretical attention to more precise determination is warranted, since experiment is incapable of determining them separately. One promising approach is the "polarization model" for water (Stillinger and David, 1978) which, in a Monte Carlo or molecular dynamics simulation application, would permit each of the three basic quantities to be computed.

V. ICE

A. Structural Description

Two forms of ice will be considered in this Section, hexagonal and cubic. The former is the normal result of freezing liquid water, while the latter can be prepared by slow vapor deposition on a very cold surface. Apparently these are the only two crystalline forms of water that can be prepared at low ambient pressure (Eisenberg and Kauzmann, 1969).

In their defect-free forms both cubic and hexagonal ices display the fourfold coordination shown earlier in Figure 2. At absolute zero the distance between neighboring oxygen atoms in these structures is about 2.74 Å, and the angles made by two of its oxygen neighbors at a central oxygen is the characteristic tetrahedral value

$$\theta_t = \arccos(-1/3)$$

$$= 109.47^\circ \ . \qquad (5.1)$$

The hydrogen bonds that connect neighboring molecules in ices Ih and Ic form closed polygons with all possible even numbers of sides, from the minimum size six. However these even polygons are shaped and arranged differently in the two crystals. Figure 4 shows and contrasts the hydrogen bond networks of the two ices. The structural relation between these forms may be viewed as resulting from 30° rotation of molecules along vertical hydrogen bonds in Figure 4 from an eclipsed configuration (hexagonal) to a staggered configuration (cubic).

Neutron diffraction studies of hexagonal D_2O ice (Peterson and Levy, 1957) show that along every O-O bond there are two possible positions for a hydrogen atom. Each is 1.01 Å from the nearer end oxygen, which is only slightly stretched compared to the free molecule O-D (or O-H) bond length 0.96 Å. In view of the weakness of hydrogen bonding compared to intramolecular covalent bonds it is reasonable only to interpret these diffraction results as indicating that the ice crystal consists of intact water molecules. Although analogous measurements have not been made for cubic D_2O ice, it is again only reasonable to assume that the same result would likewise be found in this closely related substance.

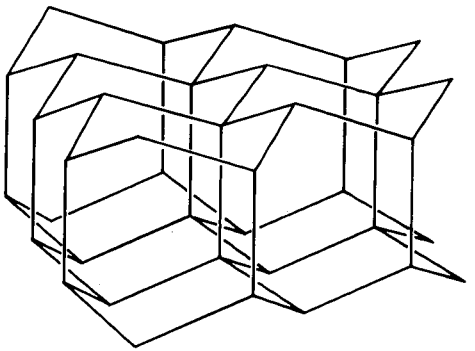

HEXAGONAL

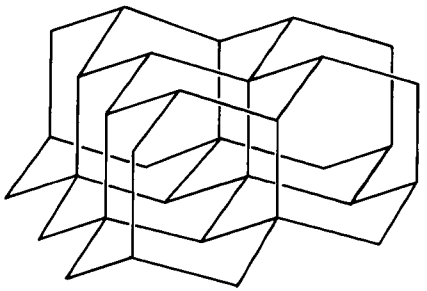

CUBIC

Figure 4. Hydrogen bond networks in hexagonal and in cubic ices. The vertices are residence positions of oxygen atoms.

The free molecule bond angle 104.45° is slightly smaller than the ideal tetrahedral angle 109.47° . However there is some theoretical evidence that hydrogen bonding

interactions tend to open up the bond angle slightly (Hankins, Moskowitz, and Stillinger, 1970) to provide a better fit to the lattice. For present purposes it will be adequate to suppose that hydrogens are essentially on the O-O axes. With two hydrogens and four bonding directions, each water molecule has six possible orientations.

Expanding upon earlier suggestions by Bernal and Fowler (1933), Pauling was the first to recognize clearly that the existence of intact water molecules in the hydrogen-bond network of ice Ih permitted multiple configurational degeneracy that was associated with proton disorder (Pauling, 1935). He formulated the following set of "ice rules" to define and restrict the possible positions of hydrogens within the crystal.

1. Along each nearest-neighbor O-O bond there is one and only one hydrogen.
2. Each hydrogen has available to it two equivalent but distinct sites, one on either side of the O-O bond midpoint.
3. Along the four bonds emanating from each oxygen vertex, precisely two bear "nearby" hydrogens, while the other two bear "distant" hydrogens (intact molecule condition).

These "ice rules" simply re-express the above interpretation of neutron diffraction observations (while historically preceding them by more than two decades!). Of course they are equally applicable to ices Ih and Ic.

Pauling estimated the number of distinct configurations permitted by the ice rules using a simple but surprisingly accurate method. He observed first that in a crystal of N molecules there are 2N bonds (neglecting surface effects). Were it not for rule 3 above, this would lead to 2 choices for each bond, or 2^{2N} configurations. However rule 3 will eliminate many of these. At each of the N oxygens only 6 of the $2^4 = 16$ ways of placing hydrogens along the four bonds satisfy this last restraint. Pauling then proposed that an attrition factor 6/16 should be incorporated for each vertex, thus leading to the following number of configurations:

$$W_N \cong 2^{2N}(3/8)^N = (3/2)^N \ . \tag{5.2}$$

Pauling furthermore suggested that the vast majority of the W_N canonical ice configurations lie sufficiently close in energy that ice would display the full proton disorder permitted by the ice rules when it is formed by freezing the liquid. This proton disorder ought then to remain "frozen" into the crystal even as the latter is cooled toward absolute zero. The Pauling entropy

$$S_P = k_B \, ln \, W_N \ , \tag{5.3}$$

using estimate (5.2) for W_N, agrees well with the residual ice entropy at O°K measured calorimetrically by Giaque and Stout (1936). Barring inadvertent contributions from other types of crystal disorder (point defects, dislocations, grain boundaries, etc.), this result strongly supports the presumption of near-degeneracy for the W_N configurations. It is from among these canonical configurations that the static dielectric response of ice to homogeneous electric fields must be calculated.

Subsequent combinatorial studies have produced more accurate values for W_N. The best are due to Nagle, who finds for both cubic and hexagonal ice (Nagle, 1966):

$$W_N \cong (1.5069)^N \ . \tag{5.4}$$

Consequently Pauling's use of independent attrition factors for each oxygen vertex leads to an underestimate, though only slightly so on a per-site basis. Details of a graphical method on which an accurate calculation of W_N can be based are contained in the later Sec.V. E.

While enumeration of the canonical ice configurations constitutes the most important structural feature of ice, a complete discussion of electrical behavior requires consideration of two types of point defects. These are the ionic defects, and the "Bjer-

rum" defects. They correspond respectively to violation of ice rules 3 and 1.

Ionic defects are produced spontaneously by the same process of molecular dissociation that operates in the liquid phase, namely

$$H_2O \rightleftarrows H^+ + OH^- \quad . \tag{5.5}$$

Successful dissociations are those for which the ionic products diffuse away from one another to avoid immediate recombination. In ice this produces a pair of separated vertices which violate rule 3 by having a missing hydrogen (OH^-), and by having an excess hydrogen (H_3O^+). This situation can exist with one hydrogen still along each O-O bond, and can be produced simply by shifting in concert a set of hydrogens along a connected bond chain between the final ionic centers. Ions are rare in pure liquid water and rarer still in pure ice, though doping the latter with HF or NH_3 allows the experimenter to vary their concentration at will within reasonable limits (Levi, Milman, and Suraski, 1963). Electrical conduction in ice proceeds only by motion of these H_3O^+ and OH^- defects, with mobility due to hopping of hydrogens from one bond position to the other to transfer the excess hydrogen ion or hydrogen ion "hole" by one lattice site.

"Bjerrum" defects are orientational violations of the ice rules, involving no dissociation, but only intact molecules (Bjerrum, 1952). These violations produce defects in pairs, with one member of the pair consisting of two hydrogens along a bond ("d" defect) and the other consisting of no hydrogens along a bond ("l" defect). Both kinds of Bjerrum defect are mobile, with molecular rotations serving to transfer the defect from one bond to another with which it shares an oxygen vertex. The concentration of d and of l defects in pure hexagonal ice at $-10°C$ is 7×10^{15} cm^{-3}, and the energy of formation of a defect pair is 0.68 eV (Fletcher, 1970). Bjerrum defects constitute the crystalline analog of broken hydrogen bonds that are conspicuously and copiously

present in the liquid phase.

Since the rotation of polar molecules (by fixed angles) is involved in the creation and movement of Bjerrum defects, it is possible to assign effective charges to them. Onsager and Dupuis (1962) derive the following expression for the charge of a d defect (equal magnitude but opposite sign is appropriate for an l defect):

$$q = 3^{1/2}\,\mu/b \quad , \tag{5.6}$$

where μ is the mean molecular moment in the crystal, and b is the O-O bond distance. Using the value 2.73 D for μ (Wörz and Cole, 1969) and 2.76 Å for b (the value appropriate for hexagonal ice near its melting point), one obtains

$$q = 1.71 \times 10^{-1} \text{ esu}$$

$$= 0.357 \text{ e} \quad . \tag{5.7}$$

On account of this charge the d and l defects will drift apart in an externally applied electric field, and the water molecules that have oriented to accommodate this drift create a polarization field in the crystal.

We should note in passing that the ice crystal is surely distorted in the immediate vicinity of any Bjerrum defect. This distortion arises from the mutual repulsion either of electron lone pairs (l defect) or of hydrogens (d defect) that point along the ice-rule-violating bond. The result will be a local dilation for both types of defect; in other words they have positive volumes of formation. This requires that increasing pressure will reduce the equilibrium concentration of Bjerrum defects. For present purposes we can disregard lattice distortion around Bjerrum defects.

B. Dielectric Formulas

The modified Kirkwood formula that was derived earlier for liquid water, Eq.

(4.27), is directly applicable to cubic ice Ic. To the extent that hexagonal since Ih may be regarded as dielectrically isotropic, we can also use the same formula to describe this more common form of the solid. There is fortunately one important simplification which apparently obtains for the ices, namely

$$\phi \cong 1 \ , \tag{5.8}$$

owing to the fact that the hydrogen bond network maintains virtually invariant connectivity. The only exceptions to this invariance will be associated with point defects which we have seen above are rare. We will proceed on the assumption that ϕ can be set equal to unity, so that the simpler version of the "Kirkwood" formula, Eq. (4.21), can be employed.

At relatively low frequencies the complex time-dependent dielectric response of ice empirically seems closely to fit the single-relaxation-time formula:

$$\epsilon(\omega) = \epsilon_\infty + \frac{\epsilon_0 - \epsilon_\infty}{1 + i\omega\tau_d} \ . \tag{5.9}$$

where for ice Ih at 0°C (Eisenberg and Kauzmann, 1969)

$$\tau_d \cong 2 \times 10^{-5} \text{ sec} \ . \tag{5.10}$$

The relaxation process involved is molecular reorientation, mediated by motion of Bjerrum defects. By fitting experimental data for $\epsilon(\omega)$ Auty and Cole (1952) find that the "infinite frequency" dielectric constant has the value

$$\epsilon_\infty \cong 3.10 \ . \tag{5.11}$$

The frequency range for which ϵ_∞ gives the dielectric response for ice is broad, spanning the interval between roughly 30 Mhz and 1 Thz (10^{-3} cm^{-1} to 30 cm^{-1}).

Even so, the electric field varies sufficiently slowly at the upper end of this range that librational motions of molecules in the lattice are able to respond fully to the external perturbation. Hence ϵ_∞ is not really the ice phase analog of the quantity ϵ_h that was introduced in Sec. IV for the liquid; this latter refers to frequencies so high that hindered rotations in the liquid could *not* respond to an exciting field. Reference to the review by Irvine and Pollack (1968) suggests that the real part of the ice Ih dielectric function at 1200 cm^{-1} (the frequency for which ϵ_h was previously identified) may be as low as 1.40 .

The structure and bonding in the ices make it natural to discuss water molecule orientations just in terms of the six discrete possibilities defined by directions to first-neighbor oxygens. This simplification relegates all hindered translational, librational, and intramolecular vibrational motion to "high frequency" response. Consequently we shall use the "Kirkwood" dielectric formula in the form

$$\frac{\epsilon_0 - 1}{\epsilon_0 + 2} = \frac{\epsilon_\infty - 1}{\epsilon_\infty + 2} + \frac{4\pi\rho\beta g\epsilon_0}{(2\epsilon_0+1)(\epsilon_0+2)} <\mu^2> \ , \tag{5.12}$$

where ϵ_∞ has the value shown in Eq. (5.11). By adopting this point of view the integral (3.20) which defines the correlation factor g reduces to a weighted sum over lattice sites and over orientations at each site:

$$g = 1 + \lim_{\omega\to\infty} \lim_{N,V\to\infty} \sum_{\mathbf{r}_{12}}^{\omega} \sum_{\mathbf{u}_1} \sum_{\mathbf{u}_2} \mathbf{u}_1 \cdot \mathbf{u}_2$$

$$\times p(\mathbf{r}_{12}, \mathbf{u}_1, \mathbf{u}_2, N, V) \tag{5.13}$$

Here p represents the probability for molecules on sites separated by displacement $\mathbf{r}_{12}$ to have discrete orientations specified by unit vectors $\mathbf{u}_1$ and $\mathbf{u}_2$ (nominally along the molecular symmetry axes). Once again we stress the importance of the ordered limits

in Eq. (5.13): *First* the system size passes to infinity, *then* the size of the region ω over which the neighbor sum is carried out is allowed to become infinite.

For later reference it will be useful to invert Eq. (5.12) to provide a value for $g<\mu^2>$. Using 3.10 for ϵ_∞, and 91.2 for ϵ_0 at 0°C (Wörz and Cole, 1969), we obtain the following result for ice Ih:

$$g<\mu^2> = 10.21\ D^2 \ . \tag{5.14}$$

In order to achieve a full understanding of the dielectric behavior of ice it is necessary to augment the "Kirkwood" dielectric formula with another due to Slater (1941) and Onsager (Onsager and Dupuis, 1960). We now derive the Slater-Onsager formula in a manner which should help to clarify its relation to the complementary "Kirkwood" result.

Consider a finite slab of ice, in single crystal form, that has been placed between parallel capacitor plates as shown in Fig. 5. By external connection to a potentiostat, there will be an electric field **E** established throughout the ice sample. We will suppose that **E** is constant and parallel to $\mathbf{u}_z$, the unit vector normal to the plates.

The macroscopic polarization **P** induced by the field **E** can be split into two parts. The first includes the response of the system to **E** without permitting molecules to change their discrete orientations:

$$\mathbf{P}_1 = (\epsilon_\infty - 1)\mathbf{E}/4\pi \ , \tag{5.15}$$

where ϵ_∞ is the same quantity used above. The remainder of **P**,

$$\mathbf{P}_2 = \mathbf{P} - \mathbf{P}_1 = (\epsilon_0 - \epsilon_\infty)\mathbf{E}/4\pi \ , \tag{5.16}$$

arises from transitions among the canonical ice structures so as to bias the orientations of molecules preferentially along **E**.

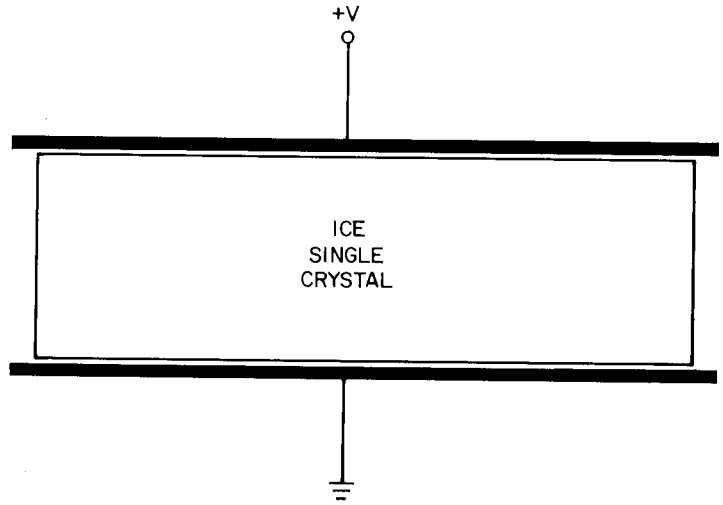

Figure 5. Parallel-plate capacitor arrangement used to derive the Slater-Onsager dielectric formula.

In order to obtain a useful expression for this second part of **P** we need to consider the statistical problem explicitly. In particular we have (since all molecules are essentially equivalent):

$$\mathbf{P}_2 = \rho<\mu^2>^{1/2} Z_N^{-1} \sum_{\{\mathbf{u}_i\}} \mathbf{u}_1 \exp(-\beta\Phi) \ ,$$

$$Z_N = \sum_{\{\mathbf{u}_i\}} \exp(-\beta\Phi) \ , \tag{5.17}$$

where the sums span all 6^N arrangements of discrete orientations. The appropriate potential Φ includes a pre-averaging over hindered translational, librational, and intramolecular vibrational motions. Furthermore Φ discourages Bjerrum defects by containing large positive contributions for ice rule violations.

We can write Φ as follows:

$$\Phi = \Phi_0(\mathbf{u}_1 \cdots \mathbf{u}_N) - <\mu^2>^{1/2} \mathbf{E} \cdot \sum_{j=1}^{N} \mathbf{u}_j \ . \tag{5.18}$$

The first term Φ_0 stands for the potential energy of the ice with $\mathbf{E} = 0$ (shorted capacitor plates), while the second term is the interaction of the molecular moments with the external field. When expression (5.18) is placed in Eqs. (5.17) and only terms linear in $\mathbf{E}$ then retained, one finds

$$\epsilon_0 - \epsilon_\infty = 4\pi\rho\beta<\mu^2> \sum_{j=1}^{N} <(\mathbf{u}_1 \cdot \mathbf{u}_z)(\mathbf{u}_j \cdot \mathbf{u}_z)> \ . \tag{5.19}$$

The averages here refer to the shorted-plate situation ($\Phi \equiv \Phi_0$). If it is legitimate to treat the ice crystal as isotropic, the last equation simplifies one step further to the Slater-Onsager equation:

$$\epsilon_0 - \epsilon_\infty = (4\pi/3)\ \rho\beta G\ <\mu^2> \ , \tag{5.20}$$

where

$$G = \sum_{j=1}^{N} <\mathbf{u}_1 \cdot \mathbf{u}_j> = N^{-1} \sum_{i,j=1}^{N} <\mathbf{u}_i \cdot \mathbf{u}_j> \ . \tag{5.21}$$

We are of course interested in the behavior of a macroscopic dielectric sample, so the large system limit is appropriate. Analogously to Eq. (5.13) above for g, we therefore write

$$G = 1 + \lim_{N,V\to\infty} \sum_{\mathbf{r}_{12}} \sum_{\mathbf{u}_1} \sum_{\mathbf{u}_2} \mathbf{u}_1 \cdot \mathbf{u}_2\ p(\mathbf{r}_{12}, \mathbf{u}_1, \mathbf{u}_2, N, V) \ . \tag{5.22}$$

Unlike the case for g, G includes *all* pair separations $\mathbf{r}_{12}$ in the system. The last Eq. (5.22) is the discrete-orientation version of the previous general Eq. (3.19).

Using the same data as before for ice Ih at 0°C, we can invert the Slater-Onsager equation (5.20) to deduce

$$G<\mu^2> = 25.89\ D^2 \ . \tag{5.23}$$

Comparing this result with Eq. (5.14) indicates that

$$G > g \ . \tag{5.24}$$

Further insight into the underlying statistical problem can be achieved by transforming the Slater-Onsager formula somewhat. We can classify configurations of the ice crystal according to their values of

$$t_z = \sum_{j=1}^{N} \mathbf{u}_j \cdot \mathbf{u}_z \ , \tag{5.25}$$

which is proportional to the z component of the total system moment in the absence of the external field. On account of the discrete set of directions available for the $\mathbf{u}_j$, the possible t_z values also form a discrete set, though these values need not be equally spaced. For any given t_z let

$$w(t_z) = \sum_{\{\mathbf{u}_i\}}{}' \exp\{\beta[<\Phi_0> - \Phi_0(\mathbf{u}_1 \cdots \mathbf{u}_N)]\} \tag{5.26}$$

where the primed sum includes only configurations which have the proper t_z value, and where

$$<\Phi_0> = \sum_{\{\mathbf{u}_i\}} \Phi_0 \exp(-\beta\ \Phi_0) / \sum_{\{\mathbf{u}_i\}} \exp(-\beta\ \Phi_0) \tag{5.27}$$

is the mean value of Φ_0 in the canonical ensemble over *all* configurations. Notice that if the Bernal-Fowler-Pauling picture is correct that all "ice-rule" configurations have equal energy, and none others occur, then $w(t_z)$ is precisely the number of canonical ice configurations with the given moment component, and so

$$W_N = \sum_{t_z} w(t_z) \quad . \tag{5.28}$$

Returning to the more general circumstance wherein available configurations may differ in energy, we can use $w(t_z)$ to rewrite $\mathbf{P}_2$ from Eq. (5.17) in the following scalar form:

$$\mathbf{P}_2 \cdot \mathbf{u}_z = \left(\frac{\rho <\mu^2>^{1/2}}{N} \right) \frac{\sum t_z \, w(t_z) \exp(\beta E <\mu^2>^{1/2} t_z)}{\sum w(t_z) \exp(\beta E <\mu^2>^{1/2} t_z)} \quad . \tag{5.29}$$

By paralleling the earlier procedure that led to the Slater-Onsager formula, we now obtain

$$\epsilon_0 - \epsilon_\infty = \left(\frac{4\pi\rho\beta <\mu^2>}{N} \right) \frac{\sum t_z^2 \, w(t_z)}{\sum w(t_z)} \quad . \tag{5.30}$$

Thus the dielectric response has been related to the second moment of w. Comparison with the Slater-Onsager expression (5.20) reveals that

$$G = \frac{3 \sum t_z^2 \, w(t_z)}{N \sum w(t_z)} \quad . \tag{5.31}$$

For the macroscopic systems of interest we can reasonably expect the central limit theorem to apply to w. That is, it should behave essentially as a Gaussian function centered about $t_z = 0$. In that circumstance it is valid asymptotically to regard $w(t_z)$ as a function of the *continuous* variable t_z and thence to replace the second moment in Eq. (5.31) by a second derivative:

$$G = -3[N \partial^2 \, ln \, w / \partial t_z^2 \, |_{t_z=0}]^{-1} \quad . \tag{5.32}$$

From Eq. (5.21) the fluctuation character of G is obvious. In the most general case

$$G = \mathrm{Tr}\, \mathbf{G} \quad ,$$

$$G_{\alpha\beta} = N^{-1} <t_\alpha \, t_\beta> \quad ,$$

$$\mathbf{t} = \sum_{j=1}^{N} \mathbf{u}_j \quad . \tag{5.33}$$

It seems unavoidable that this mean-square fluctuation quantity (to be computed in the absence of external fields) must depend in a fundamental way on electrostatic boundary conditions. Thus far we have supposed that the surfaces of the ice slab were held at constant potential, and in particular the fluctuation (5.33) giving G refers to constant potential at the entire boundary. This circumstance amounts to surrounding the crystal with a metallic conductor. Any surface charges which might occur are automatically neutralized by induced image charge in the conductor. But if that surrounding conductor is absent (*i.e.* a crystal in free space), any surface charge density remains unneutralized and produces an electric field within the crystal. The field energy that results is positive and will tend to diminish the magnitude of surface-charge-producing fluctuations. Consequently the tensor components $G_{\alpha\beta}$ will depend on boundary conditions, and will be dependent on the shape of the sample.

It is only by invoking conducting boundary conditions that surface charge effects are eliminated, and thus shape dependence is eliminated. Clearly these are the boundary conditions of choice for further statistical study of the dielectric behavior of ice, at least within the context of the Slater-Onsager formula. The resulting cancellation of surface charge apparently permits one to neglect long-range molecular interactions in ice, and creates the only situation in which the Pauling ice rules and resulting degeneracy may consistently be employed for the study of static dielectric response.

C. Square Ice

In order to aid in understanding the configurational statistics of hydrogen disorder in ice, it has been helpful to examine a two-dimensional "square ice" model (Meijering, 1957; DiMarzio and Stillinger, 1964). This model retains fourfold hydrogen bond coordination of the real three dimensional ices, but does so by placing oxygens at the vertices of a square planar lattice. The smallest hydrogen bond polygon thus is a square, in contrast to hexagons in ices Ic and Ih. In order to maintain the possibility of six discrete arrangements for a water molecule at each vertex, the molecules are permitted to be either straight or bent. Figure 6 shows a typical configuration of square ice obeying the usual ice rules, and conforming to periodic boundary conditions in both directions.

Square ice exhibits proton disorder just as do the three dimensional ices. The earlier Pauling argument applies without modification to the present case and consequently leads to the same estimate [Eq. (5.2)] for the degeneracy W_N of an N-molecule sample.

Since the pedagogical value of square ice pertains strictly to the combinatorial problem of proton disorder, these is no sense to attributing high frequency response to the model. Instead only molecular moments are postulated to interact with the "external field" $\mathbf{E}$ to give an energy of the form:

$$-\mathbf{E} \cdot \sum_{j=1}^{N} \mu_j \ . \tag{5.34}$$

Straight molecules naturally have vanishing moments. Bent molecules have moments pointing along the molecular right-angle bisector with a fixed magnitude denoted by μ_b.

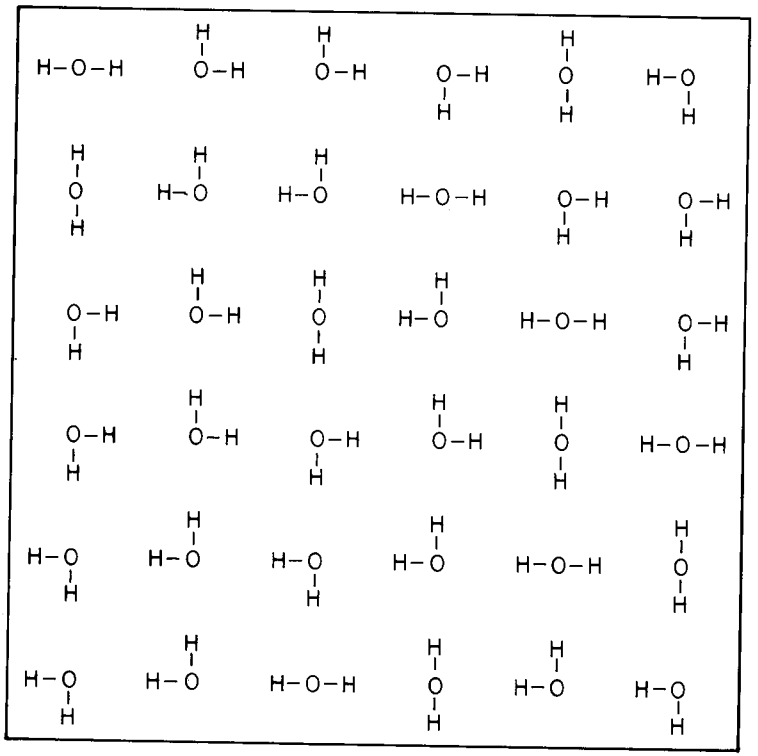

Figure 6. Typical defect-free configuration of square ice. Periodic boundary conditions apply; the unit cell shown can bond perfectly at the boundaries to periodic replicas of itself.

If ρ stands for the areal density of molecules in the square ice, then the mean polarization induced by $\mathbf{E}$ is:

$$\mathbf{P} = \rho \sum \mu_1 \exp(\beta \mathbf{E} \cdot \sum_{j=1}^{N} \mu_j)/Z_N^{(2)}(\mathbf{E}) \ ,$$

$$Z_N^{(2)}(\mathbf{E}) = \sum \exp(\beta \mathbf{E} \cdot \sum_{j=1}^{N} \mu_j) \ . \tag{5.35}$$

The sums cover all canonical configurations which, in the absence of **E**, are presumed to have identical energies. In the linear response regime **P** will be parallel to **E** (isotropic response) with a proportionality that may be taken to define the two-dimensional dielectric constant:

$$\mathbf{P} = (\epsilon_0 - 1)\mathbf{E}/4\pi \quad . \tag{5.36}$$

By utilizing Eq. (5.35) in first order in **E**, one subsequently obtains the Slater-Onsager formula for square ice:

$$\epsilon_0 - 1 = 2\pi\beta\rho G\langle\mu^2\rangle \quad , \tag{5.37}$$

where (passing to the large system limit)

$$G = \lim_{N\to\infty} \sum_{j=1}^{N} \langle\boldsymbol{\mu}_1 \cdot \boldsymbol{\mu}_j\rangle/\langle\mu^2\rangle \quad , \tag{5.38}$$

and where the average values refer to vanishing **E**.

A dielectric formula of the Kirkwood type cannot unambiguously be derived for the present two-dimensional case. Nevertheless a quantity g can directly be defined to compare with G:

$$g = 1 + \lim_{\omega\to\infty} \lim_{N\to\infty} \sum_{j=2}^{(\omega)} \langle\boldsymbol{\mu}_1 \cdot \boldsymbol{\mu}_j\rangle/\langle\mu^2\rangle \quad . \tag{5.39}$$

As before, the summation (over j) spans a fractionally small subregion ω of the entire system. Only after the system size becomes infinite is this region ω surrounding site 1 permitted to become infinite.

Suppose that x and y are Cartesian coordinates whose axes are parallel to the principal directions of the square ice model. Because the two directions are equivalent in the field-free case, and because all molecules are at equivalent sites when periodic

boundary conditions are employed, we can write

$$G\langle\mu^2\rangle = \lim_{N\to\infty} (2/N) \sum_{i,j=1}^{N} \langle\mu_{ix}\, \mu_{jx}\rangle \quad . \tag{5.40}$$

If the square lattice consists of an n × n array ($N = n^2$), it will be convenient to collect terms in expression (5.40) by columns of n molecules. Hence set

$$s_{\alpha x} = \sum_{i\epsilon\alpha} \mu_{ix} \qquad (1 \leq \alpha \leq n)) \tag{5.41}$$

where α serves as a column index. Then

$$G\langle\mu^2\rangle = \lim_{n\to\infty} (2/n^2) \sum_{\alpha,\gamma} \langle s_{\alpha x}\, s_{\gamma x}\rangle \quad . \tag{5.42}$$

The moment μ_j of any molecule j may be thought of as composed of separate "bond moments" pointing along its two covalent OH bonds. Hence μ_{jx}, the horizontal component of μ_j, is associated with horizontal OH bonds in that molecule. since μ_b is the magnitude of the moment of a bent molecule it is easy to see that

$$s_{\alpha x} = 2^{-1/2}\, \mu_b(n_r - n_l) \quad , \tag{5.43}$$

where n_r and n_l respectively give the numbers of horizontal OH bonds pointing right and pointing left. A glance at Fig. 6 reveals a fundamental conservation law generated by the ice rules, namely that the quantities n_r and n_l are identical for all columns. Hence all $s_{\alpha x}$ are equal for any configuration of square ice obeying the ice rules. This in turn allows us to rewrite Eq. (5.42) in the following way:

$$G\langle\mu^2\rangle = 2 \lim_{n\to\infty} \langle s_x^2\rangle \quad , \tag{5.44}$$

where s_x represents the common value of all $s_{\alpha x}$.

Simultaneous equality of all $s_{\alpha x}$ across the planar array is a manifestation of configurational "stiffness" that results from the ice rules. A closely related result may also be obtained by studying diagrams such as Fig. 6. Consider any strip of m contiguous horizontal rows of molecules, where $0<m<n$. Then proceeding from left to right, the numbers of horizontal OH bonds pointing right (or pointing left) in vertical bond columns within the strip can change only by -1, 0, or +1. This restraint severely restricts the ability of the system to "forget" the polarization pattern present in any vertical column in passing from one column to the next. In particular an uninterrupted vertical run of $m = 2l$ right-pointing OH bonds in one column cannot be "smoothed out" in less than l horizontal steps between columns; on the average it would be expected that even greater spatial persistence of such a configurational fluctuation would obtain.

Of course everything stated for horizontal bonds in columns and in horizontal strips is equally valid for vertical bonds in rows and in vertical strips, owing to fundamental equality of the x and y directions.

The configurational stiffness of the ice rules leads one to suspect that in the infinite system limit rather long-range correlations are present in the quantities $<\mu_1 \cdot \mu_j>$. In this respect we can anticipate a basic difference between square ice and the corresponding planar Ising models. For the latter (at least above their critical points) the spin-spin correlation functions are short-ranged, with exponential damping as distance r_{1j} increases (Stanley, 1971). By contrast, calculations by Sutherland (1968) for general two-dimensional hydrogen-bonded ferroelectric models imply that correlations in defect-free ice along a given direction should vary as r_{1j}^{-2}. Occasional ice rule violations, in the form of Bjerrum d and l defects, would however relax the configurational stiffness, and ought to shorten the range of configurational correlations in square ice by introducing exponential damping.

A major theoretical advance occurred when Lieb showed that the configurational counting problem for square ice could be solved exactly (Lieb, 1967a,b). Lieb's method involves finding a transfer matrix representation for the problem analogous to that for the square Ising model (Kramers and Wannier, 1941) and then finding eigenvalues and eigenvectors for the transfer matrix. the details are beyond the scope of this article, so the interested reader is referred to the original papers. The final result is

$$\lim_{N\to\infty} (W_N)^{1/N} = (4/3)^{3/2}$$

$$= 1.539\ 600\ 718\ \cdots\ . \qquad (5.45)$$

This indicates that square ice actually enjoys slightly greater configurational freedom than that suggested by the Pauling estimate (1.500 ...) for the same quantity. It is worth noting in passing that Onsager and Dupuis (1960) have demonstrated that the Pauling estimate is always a lower bound on the exact result regardless of the dimension of the model under consideration.

The square ice model is just one member of an extensive family of related two-dimensional models for hydrogen-bonded crystals that can be solved exactly by transfer matrix diagonalization. An article by Lieb and Wu (1972) provides a comprehensive account of this general area.

Straight molecules of both orientations represent one-third of the six permitted molecular configurations in square ice. On an *a priori* basis one might have guessed that their relative concentration correspondingly ought to be one-third. In fact they occur with higher than *a priori* frequency. Using the exact solution method Lieb and Wu (1972, p. 450) find the straight-molecule fraction to be

$$3^{1/2}\left(\frac{3}{2} - \frac{1}{\pi}\right) - \frac{5}{3} = 0.380\ 080\ 649\ 3\ldots\ . \qquad (5.46)$$

From this we immediately find that

$$<\mu^2> = \left[\frac{8}{3} - 3^{1/2}\left(\frac{3}{2} - \frac{1}{\pi}\right)\right]\mu_b^2$$

$$= 0.619\,919\,350\,7\ldots\,\mu_b^2 \ . \qquad (5.47)$$

Nagle (1974) has pointed out that an exact value for square-ice G can be extracted from a generalization of the Lieb solution that has been published by Sutherland, Yang, and Yang (1967). The result is the following:

$$G = 6\,\mu_b^2/\pi<\mu^2>$$

$$= 3.080\,819\,005\,\cdots \ . \qquad (5.48)$$

The reader must be warned that Nagle (1974) has employed a different convention for his definition of G; the relation of his quantity G_N to ours is:

$$G_N = 3<\mu^2>G/2\mu_b^2$$

$$= 9/\pi = 2.864\,788\,976\,\cdots \ . \qquad (5.49)$$

Unfortunately no comparable exact result is available for the square-ice g, Eq. (5.39).

D. Monte Carlo Simulations

With the advent of rapid digital computers it has become possible to augment theory of many body systems with "numerical experiments", which serve to simulate the phenomena of interest. This type of activity has been applied to hydrogen-bond statistics in ice, including both two and three dimensional cases. The results that have emerged provide an important contribution to the present subject.

The first ice-model simulations were reported by Rahman and Stillinger (1972). These authors (RS) examined local correlations in both cubic and hexagonal ices, subject to the Bernal-Fowler-Pauling configurational rules. For cubic ice a crystal comprising 4096 molecules was used; for hexagonal ice the corresponding number was 2048. In both cases periodic boundary conditions were imposed in order to eliminate specific surface effects. The objective of the RS study was to evaluate the Kirkwood factor g and to show how this quantity was built up of contributions from successive shells of neighbors in the respective crystals. Strictly speaking the definition of g, Eq. (5.13), would require consideration of infinitely large crystals. This is obviously impossible in any simulation, so implicit in the choice of system size is the presumption that the limiting behavior can be extracted from given calculations with satisfactory accuracy. Subsequent studies (see below) seem to show that the RS choices for crystal sizes are acceptable in this regard.

The procedure devised by RS to sample canonical ice configurations required first that an appropriate starting configuration be constructed which satisfied the ice rules, as well as the periodic boundary conditions. Then a random ("Monte Carlo") procedure for executing transitions between canonical configurations, consistent with the boundary conditions, was implemented. The required orientational probabilities were subsequently calculated as averages over a long sequence of the crystal configurations generated.

In order to produce transitions closed polygonal paths connecting bonded neighbors were found, by a random search procedure, along which all covalent OH bonds had the same direction. Having identified such a closed oriented path it is then possible to shift all hydrogens simultaneously to their alternate bond positions. This leaves OH covalent bonds with the reverse direction everywhere a long the closed path. Ice rules are still obeyed after the shift, for each molecule along the path gains back a hydrogen

after having lost one. Figure 7 indicates several such a shifts for hydrogens in the pictorially convenient two-dimensional square ice analog, starting with the configuration of Fig. 6. It is possible to show that this procedure in the long run samples all canonical ice configurations uniformly.

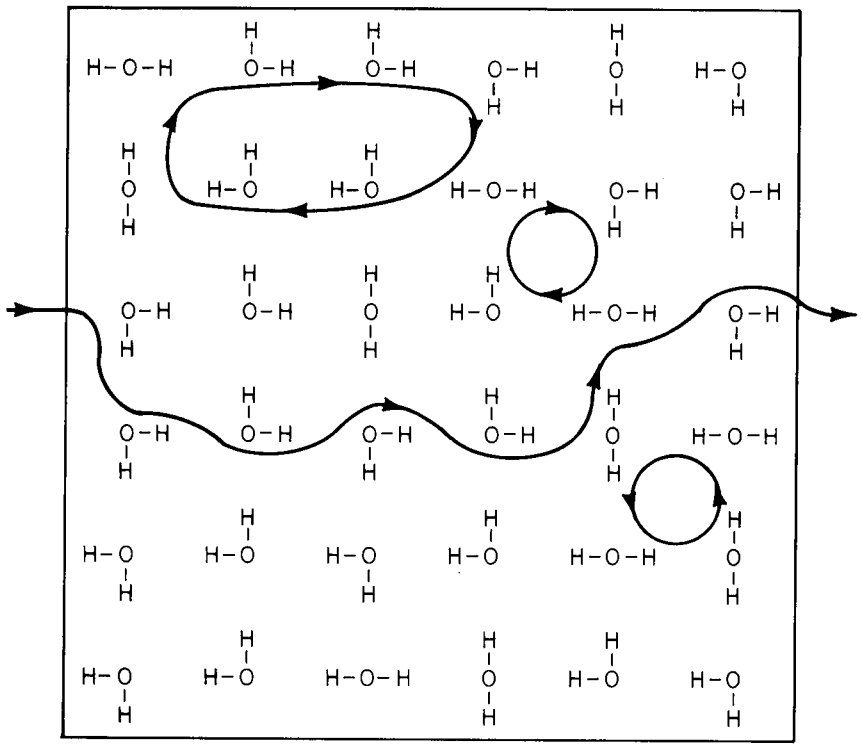

Figure 7. Possible hydrogen shifts around polygonal paths to generate a new canonical configuration. In addition to simple closed paths (three shown) the periodic boundary conditions permit paths to exist which connect molecules with their images (one shown, running left to right).

The computer-implemented search for closed oriented paths tends predominately to find short paths. The greater the number of steps involved the less likely it is to be identified in a reasonable amount of computing time. Thus hexagonal paths were the species most frequently obtained in the RS calculation. For large crystals (as in the RS study) the chance of obtaining paths that entirely span the system from one molecule to its periodic image (see Fig. 7) is very small. Consequently RS eliminated such occurrences from the outset, and utilized only the simple paths (three shown in Fig. 7) which avoid images of particles already visited.

In both the hexagonal and cubic ice models examined by RS, the initial configurations were selected to have zero net moment. Transitions which are restricted to image-avoiding paths can never change the system moment, so in fact the RS calculations only sample the zero moment subspaces of the entire set of Bernal-Fowler-Pauling configurations. For this reason no information about the global quantity G can be obtained, but useful results for the more localized quantity g can still be inferred.

The basic results obtained are the quantities

$$g_0^{(\nu)} = n_\nu \langle \mathbf{u}_1 \cdot \mathbf{u}_j \rangle \quad . \tag{5.50}$$

Here molecule j is one of the n_ν which form the ν-th coordination shell surrounding molecule 1. As before the $\mathbf{u}$'s denote unit vectors along the molecular symmetry axes. The subscript "0" in Eq. (5.50) indicates that the average has been calculated only over the zero-net-moment subspace. Table I shows the RS results for cubic ice, giving the shell radii, the n_ν, and the $g_0^{(\nu)}$ for $0 \leq \nu \leq 25$. A sequence of approximately 50,000 configurations was produced for this calculation, of which 1 in every 200 was utilized for the purpose of calculating averages. Of course for each configuration *all* pairs of molecules of a given separation were interrogated in producing the averages.

Shells 1 through 25 surrounding a chosen molecule in cubic ice comprise 524 neighbors, a not insignificant fraction of the entire 4095 in all shells. The zero-moment restraint imposed by RS requires that the entire collection of 4095 neighbors have a net moment equal in magnitude but antiparallel to that of the central molecule. Under the assumption that this moment is on average equally distributed over all 4095 neighbors, we can see that the $g_0^{(\nu)}$ shown in Table I for $\nu > 0$ must have been diminished accordingly. By the same reasoning the natural mean moment of the first, second, ... shells of neighbors must be cancelled by a moment distributed over the entire system. From this point of view it is elementary to show that the properly corrected shell correlation quantities for $\nu > 0$ ought to be given by

$$g^{(\nu)} = g_0^{(\nu)} + n_\nu (N - N_\omega)^{-1} \sum_{\nu=0}^{25} g_0^{(\nu)} \ ,$$

$$N = 4096 \ , \qquad N_\omega = \sum_{\nu=0}^{25} n_\nu = 525 \ . \tag{5.51}$$

These corrected values are also shown in Table I. They represent the best estimates of the $g^{(\nu)}$ for an infinite unconstrained system.

Comparison of entries in the last two columns in Table I shows that the correction procedure (5.51) seems to have improved the convergence of the shell correlation factors to zero with increasing shell radius. However the correlations are rather long ranged, consistent with our earlier discussion of configurational "stiffness" in defect-free ice. On account of the oscillatory behavior of the $g^{(\nu)}$ it seems reasonable to use just the first twenty five shells to form a numerical estimate for the cubic ice g:

$$g \cong 1 + \sum_{\nu=1}^{25} g^{(\nu)}$$

$$= 2.11 \ . \tag{5.52}$$

TABLE I. Coordination shell correlation parameters for cubic ice according to Rahman and Stillinger (1972).

ν	r_ν^2/r_1^2	n_ν	$g_0^{(\nu)}$	$g^{(\nu)}$
0	0	1	1.0000	1.0000
1	1	4	1.2643	1.2664
2	8/3	12	.0032	.0094
3	11/3	12	−.4537	−.4475
4	16/3	6	.0050	.0081
5	19/3	12	.2881	.2943
6	8	24	−.0112	.0012
7	9	16	−.0825	−.0743
8	32/3	12	−.0039	.0023
9	35/3	24	−.0861	−.0737
10	40/3	24	−.0094	.0030
11	43/3	12	.0601	.0663
12	16	8	−.0009	.0032
13	17	24	.0056	.0180
14	56/3	48	−.0185	.0062
15	59/3	36	−.0330	−.0145
16	64/3	6	−.0023	.0008
17	67/3	12	−.0155	−.0093
18	24	36	−.0147	.0038
19	25	28	−.0250	−.0106
20	80/3	24	−.0129	−.0005
21	83/3	36	.0209	.0394
22	88/3	24	−.0149	−.0025
23	91/3	24	−.0140	−.0016
24	32	24	.0035	.0159
25	33	36	−.0140	.0045

Rahman and Stillinger conservatively estimated this value to be accurate within ±0.10 of the exact g for cubic ice.

The corresponding hexagonal ice calculations involved a somewhat longer sequence of configurations, roughly 140,000, from which once again every two-hundredth was used to evaluate shell averages. Results are shown for $0 \leq \nu \leq 26$ in Table II. The

TABLE II. Coordination shell correlation parameters for hexagonal ice according to Rahman and Stillinger (1972).

ν	r_ν^2/r_1^2	n_ν	$g_0^{(\nu)}$	$g^{(\nu)}$
0	0	1	1.0000	1.0000
1	1	4	1.2573	1.2613
2	8/3	12	.0546	.0667
3	25/9	1	−.0952	−.0942
4	11/3	9	−.3403	−.3312
5	16/3	6	−.0936	−.0875
6	49/9	6	.0245	.0306
7	19/3	9	.2138	.2229
8	64/9	2	−.0025	−.0005
9	8	18	.0436	.0618
10	9	9	−.0538	−.0447
11	88/9	12	−.0135	−.0014
12	89/9	3	−.0217	−.0187
13	32/3	6	−.0025	.0036
14	97/9	6	.0148	.0209
15	35/3	18	−.0681	−.0499
16	113/9	3	−.0180	−.0150
17	40/3	12	−.0455	−.0334
18	121/9	7	.0149	.0220
19	43/3	3	.0137	.0167
20	136/9	12	−.0140	−.0019
21	137/9	6	.0006	.0067
22	16	6	.0062	.0123
23	145/9	6	.0110	.0171
24	152/9	6	−.0022	.0039
25	17	12	−.0110	.0011
26	160/9	12	−.0164	−.0043

same type of procedure as before was utilized to correct the quantities $g_0^{(\nu)}$ for the influence of the zero-moment constraint on the system as a whole. The final result for the Kirkwood orientational correlation factor is

$$g \cong 1 + \sum_{\nu=1}^{26} g^{(\nu)}$$

$$= 2.065 \ , \tag{5.53}$$

for which RS suggest an uncertainty of ±.02. Considering both uncertainties, the RS calculations suggest that g's for the two three-dimensional ices are indistinguishably close to one another.

In view of the fact that hexagonal ice is inherently anisotropic it is important to resolve contributions to the quantity g along the principal axes of the crystal. For any given neighbor correlation we can write

$$g^{(\nu)} = 2g_b^{(\nu)} + g_c^{(\nu)} \tag{5.54}$$

where for example if $\mathbf{u}_b$ is a unit vector in the basal plane then

$$g_b^{(\nu)} = <(\mathbf{u}_l \cdot \mathbf{u}_b)(\mathbf{u}_j \cdot \mathbf{u}_b)> \ . \tag{5.55}$$

An analogous expression obtains for $g_c^{(\nu)}$. The respective sums over shells then resolve the full quantity g into components $2g_b$ and g_c. Rahman and Stillinger obtained the following results from their hexagonal ice Monte Carlo study:

$$g_b = 0.707 \ ,$$

$$g_c = 0.653 \ . \tag{5.56}$$

The difference between these numbers is probably outside statistical uncertainty, but seems to contradict the controversial suggestion (Humbel, Jona, and Scherrer, 1953) that the basal plane dielectric constant ϵ_b is less than that for the c axis, ϵ_c, as indicated above in Eq. (2.20).

More recently Yanagawa and Nagle (YN) have applied the Monte Carlo simulation technique to the square ice model (Yanagawa, 1979; Yanagawa and Nagle, 1980). This was an important step for two reasons. First, it permits a calibration of the precision of the Monte Carlo technique against rigorous results that have emerged from the exact analytical solution to this problem. Second, it is feasible to carry out computations both with and without the zero-net-moment constraint that was forced upon the three-dimensional RS calculations. This latter feature permits an assessment of the RS correction procedure, Eq. (5.51), and also permits evaluation of *both* g and G.

Three different system sizes were examined in the YN work, 8×8, 12×12, and 16×16, with periodic boundary conditions always applicable. Although the numbers of particles present in these systems are substantially less than those of the RS study, the linear dimensions of the respective systems are more nearly comparable. For example, the cube root of the number of molecules used in the RS simulation of cubic ice, $(4096)^{1/3}$, is just 16. The ability to utilize a relatively smaller number of molecules in examining square ice is an obvious computational advantage.

The YN study generated 100,000 configurations for each of the 8×8 and 12×12 systems, whereas 160,000 configurations were generated for the 16×16 case. Averages were computed using every twenty-fifth configuration.

The first test that must be passed by a simulation of square ice is that it produces the correct fractions of straight and bent molecules. Yanagawa and Nagle find that these fractions are slightly dependent on system size. When they extrapolate their results to infinite system size their calculations imply

$$<\mu^2>/\mu_b = 0.620 \pm 0.003 \ . \tag{5.57}$$

[Note that owing to different normalization than that employed here, YN's self correlation function "$g^{(0)}$" is 3/2 times this quantity.] This stands in excellent agreement

with the exact result Eq. (5.47) and supports the overall validity of the YN Monte Carlo procedure.

The second test concerns the global correlation quantity G, for which the exact value was stated above in Eq. (5.48). For their largest system YN find

$$G_N = 2.86 \pm 0.11 \tag{5.58}$$

or equivalently

$$G = 3.08 \pm 0.12 \ . \tag{5.59}$$

Again excellent agreement obtains.

Separate shell correlations were evaluated by YN both with and without the zero-moment constraint. The respective quantities can be denoted by $g_0^{(\nu)}$ and $g_P^{(\nu)}$. Both require corrections to yield accurate estimates of the infinite system quantities $g^{(\nu)}$. Equation (5.51) above displays the procedure to be used for $g_0^{(\nu)}$. Following the same line of reasoning the corresponding correction procedure to be applied to the $g_P^{(\nu)}$ is the following:

$$g^{(\nu)} = g_P^{(\nu)} + n_\nu (N - N_\omega)^{-1} \left[\left(\sum_{\nu=0} g_P^{(\nu)} \right) - G \right] \ . \tag{5.60}$$

Yanagawa and Nagle find that essentially identical values for $g^{(\nu)}$ are obtained from the constrained and from the unconstrained calculations, but *only* if the respective corrections are applied. This consistency gives credence to the general correction procedure.

Table III provides a few of the $g^{(\nu)}$ extracted from the YN simulation. By examining their results for all coordination shells out to large distances they conclude that

$$g = 1.6 \pm .3 \ . \tag{5.61}$$

TABLE III. Coordination shell correlation parameters for square ice according to Yanagawa and Nagle (1980).

ν	r_ν^2/r_1^2	n_ν	$g^{(\nu)}$
0	0	1	1.000
1	1	4	.826
2	2	4	−.342
3	4	4	.138
4	5	8	−.069
5	8	4	−.028

Recalling Eq. (5.48) it is evident for square ice without defects that

$$g < G \ . \tag{5.62}$$

E. Graphical Expansion Method

There is no reason to suppose that the exact Lieb solution for square ice can ever be extended to the three-dimensional ices. Consequently a need exists for a systematic technique to study orientational statistics in the ices that is broad enough to cover both two and three dimensional cases with reliability, if not rigor. A family of graphical expansions has been developed for this purpose. The initial work in this area was published by DiMarzio and Stillinger (1964). Nagle (1966, 1968, 1974) substantially simplified and extended the method. Gobush and Hoeve (1972) apparently first applied the graphical approach to the dielectric problem. In the following development

we shall follow the specific expansion procedure devised by Stillinger and Cotter (1973).

The six configurations available to a water molecule at site i in a two or three dimensional crystal will be denoted by the parameter ξ_i. Consider then the following bond function B_b for a nearest neighbor pair of sites i and j:

$$B_b(\xi_i, \xi_j) = \exp(-\beta w)/D \quad \text{(0 or 2 hydrogens along bond)}$$

$$= \exp(\beta w)/D \quad \text{(1 hydrogen along bond)} \ ,$$

$$D = \exp(-\beta w) + \exp(\beta w) \ . \tag{5.63}$$

This associates an energy 2w with those ice-rule-violating configurations specified by ξ_1 and ξ_2 which place 0 or 2 hydrogens along the same bond (in other words with *l* and d Bjerrum defects).

The product of bond functions for all 2N nearest neighbor bonds in the crystal provides a suitable generating function for the configurational problem:

$$F(\xi_1 \cdots \xi_N) = \prod_{b=1}^{2N} B_b(\xi_{i(b)}, \xi_{j(b)}) \ . \tag{5.64}$$

Strict adherence to the ice rules obtains as $w \to +\infty$, for then F is exactly 1 or 0 according to whether those rules are obeyed or violated. More generally we are able to accommodate Bjerrum orientational defects in Eq. (5.64) with finite w, but it must be kept in mind that no interaction energy between those defects will be included in this treatment in spite of the fact that they bear an electrostatic charge [Eq. (5.6)].

Orientational averages may be computed using F as the configurational weight, for example:

$$<\mu_1 \cdot \mu_j> = W_N^{-1} \sum_{\xi_1 \cdots \xi_N} \mu_1(\xi_1) \cdot \mu_j(\xi_j) F(\xi_1 \cdots \xi_N) \ ,$$

$$W_N = \sum_{\xi_1 \cdots \xi_N} F(\xi_1 \cdots \xi_N) \ . \qquad (5.65)$$

The objective now is to evaluate these general expressions in terms of a graphical expansion that is valid in principle for any w, and then to select w to fit the physical fact of very low Bjerrum defect concentration.

It will be convenient to set

$$B_b(\xi_i, \xi_j) = \tfrac{1}{2} \{1 + \lambda \, a_b(\xi_i, \xi_j)\} \ ,$$

$$\lambda = \tanh(\beta w) \ , \qquad (5.66)$$

where a_b is +1 or -1 for orientations that obey or violate ice rules respectively. λ is the fundamental expansion parameter of this graphical technique which must ultimately be set equal to a value just less than +1.

Before proceeding to details of the λ expansions it will be useful to note some symmetry properties. Because the *tanh* function is odd, changing the sign of λ is the same as changing the sign of the energy w. This exchanges the roles of bonds which obey and which violate ice rules. Because square, cubic, and hexagonal ices each have only even closed polygonal bond paths, their configurations can always be paired in such a way that any "obeying" bond in one configuration is replaced by a "violating" bond in the other and *vice versa*. This equivalence relation is achieved simply by reversing configurations of molecules at every other site. Consequently $W_N(\lambda)$ must be an even function of λ, and the special case

$$W_N(-1) = W_N(+1) \qquad (5.67)$$

shows that the number of canonical ice configurations everywhere satisfying the ice rules is precisely equal to the number of "anti-ice" configurations everywhere violating those rules.

The corresponding statements for the correlation quantities $<\mu_1 \cdot \mu_j>$ depend on whether the sites involved lie on the same or on different sublattices. If they lie on the same sublattice (so they are separated by an even number of bonds) the average is even in λ. If they lie on different sublattices (and thus are separated by an odd number of bonds) the average is odd in λ.

Figure 8 shows an anti-ice configuration for the square model, obtained from the configuration shown earlier in Figure 6 by the alternating reversal operation. A general feature of these anti-ice configurations is obvious, namely that they all have vanishing moments. This is due to the antiparallel pairing of O-H units along doubly occupied bonds with resulting cancellation of bond moments. Precisely the same pairing and cancellation occurs in the two three-dimensional ices when $\lambda = -1$. As a result it is clear for all three cases that

$$G(-1) = 0 \ . \qquad (5.68)$$

Although it is not immediately obvious that there is a corresponding simple result for g(-1), we will argue below that this quantity also vanishes.

Nagle (1968) has pointed out that the quantity a_b can be factored:

$$a_b(\xi_i, \xi_j) = -C_{ij}(\xi_i) \, C_{ji}(\xi_j) \ , \qquad (5.69)$$

where $C_{ij}(\xi_i)$ is +1 if ξ_i specifies a hydrogen along the bond, -1 if not. Consequently

$$F(\xi_1 \cdots \xi_N) = 2^{-2N} \prod_{\text{bonds}} \{1 - \lambda C_{ij}(\xi_i) \, C_{ji}(\xi_j)\} \ , \qquad (5.70)$$

and so

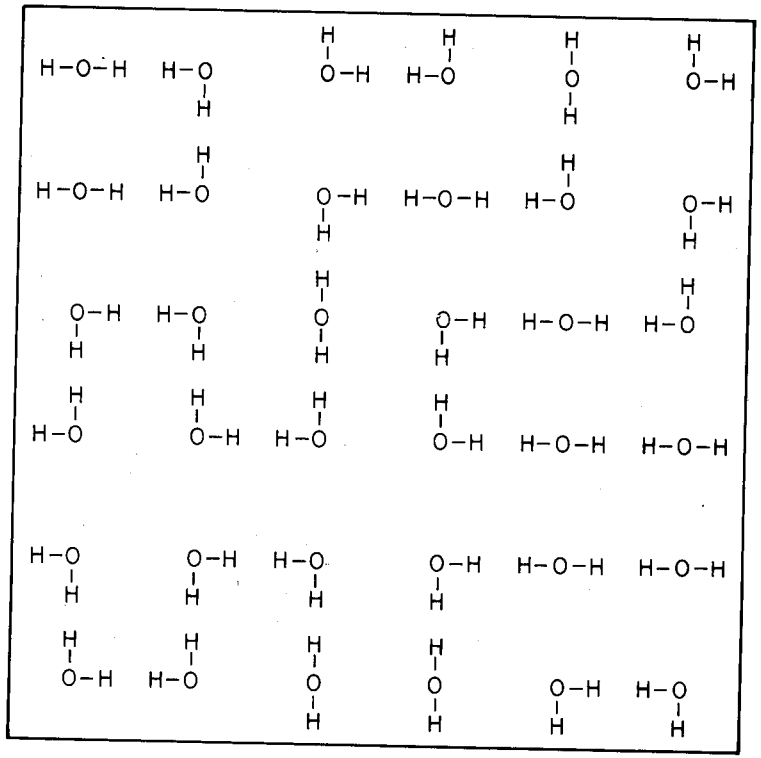

Figure 8. Anti-ice configuration. This structure was obtained from that of Figure 6 by reversing the configuration of every other molecule.

$$W_N(\lambda) = (3/2)^N \sum_{\xi_1 \cdots \xi_N} 6^{-N} \prod_{\text{bonds}} \{1 - \lambda C_{ij}(\xi_i)\, C_{ji}(\xi_j)\} \ . \qquad (5.71)$$

It is significant that the Pauling estimate for $W_N(\pm 1)$, namely $(3/2)^N$, has been isolated as a leading factor in this last expression. Systematic corrections to that estimate will be secured in ascending orders in λ. In the case of the transformed version of the correlation quantities shown earlier in Eq. (5.65) the Pauling factors cancel between

numerator and denominator to yield:

$$\langle \mu_1 \cdot \mu_j \rangle = \frac{\sum_{\xi_1 \cdots \xi_N} 6^{-N}\, \mu_1 \cdot \mu_j \prod_{\text{bonds}} \{1 - \lambda C_{ik}(\xi_i)\, C_{ki}(\xi_k)\}}{\sum_{\xi_1 \cdots \xi_N} 6^{-N} \prod_{\text{bonds}} \{1 - \lambda C_{ik}(\xi_i)\, C_{ki}(\xi_k)\}} \ . \qquad (5.72)$$

We first examine $W_N(\lambda)$, Eq. (5.71). Upon expanding the product of bond factors the separate terms generated may be put into correspondence with linear graphs on the given lattice. A bond is drawn between vertices i and j if $-\lambda C_{ij}C_{ji}$ is present in the term considered, otherwise they remain unconnected. The λ order of any term obviously equals the number of bonds in its graph. The admissible graphs connect only nearest neighbor vertex pairs since only these have bond functions in Eq. (5.71). The correspondence between terms generated by the expansion and graphs with nearest neighbor links is one-to-one.

It is easy to show that graphs containing an odd vertex (one upon which one or three bonds impinge) each contribute nothing to $W_N(\lambda)$. This arises from the facts that

$$\sum_{\xi_i} C_{ij}(\xi_i) = 0 \ ,$$

$$\sum_{\xi_i} C_{ij}(\xi_i)\, C_{ik}(\xi_i)\, C_{il}(\xi_i) = 0 \ . \qquad (5.73)$$

The only surviving terms are those whose graphs have vertices all of even order (zero, two, or four bonds impinging). This reduction in number of graphs that must be considered substantially simplifies the problem at hand.

Of those terms in W_N that remain, the simplest are those corresponding to single closed polygons on an otherwise empty lattice. More complicated terms will have graphs with several distinct bond polygons, and possibly intersecting polygons. It can

be shown (Nagle, 1966, 1968) that the value to be assigned to any given graph [before including the common factor $(3/2)^N$] is equal to $\lambda^n/3^{p_2}$, where n is the number of bonds in the graph, and p_2 is the number of vertices of order two.

As the graph order n increases so does the difficulty of graph enumeration. For present purposes we disregard details, while referring the interested reader to the original papers (Nagle, 1966; Stillinger and Cotter, 1973). The final result obtained for cubic ice can be put into the following form:

$$W_N(\lambda) = \{(3/2)[1 + 2(\lambda/3)^6 + 3(\lambda/3)^8 + 24(\lambda/3)^{10} + 167(\lambda/3)^{12} + 876(\lambda/3)^{14} + 0(\lambda^{16})]\}^N \quad . \tag{5.74}$$

The occurrence only of even powers in λ is demanded by the above-mentioned fact that W_N is even in λ. Considering just the explicitly shown terms for $\lambda = 1$, the implied numerical value is:

$$W_N(1) \cong \{(3/2)[1 + 2.7435 \times 10^{-3} + 4.5725 \times 10^{-4} + 4.0644 \times 10^{-4} + 3.1424 \times 10^{-4} + 1.8315 \times 10^{-4}]\}^N = \{1.506157\}^N \quad . \tag{5.75}$$

The series involved appears to be convergent, though not rapidly so. It seems fair to suppose that higher order terms in Eq. (5.74) would also have positive coefficients so as to bring $W_N(1)$ up to Nagle's estimate quoted earlier in Eq. (5.4).

Systematic studies of the corresponding $W_N(\lambda)$ series for square ice and for hexagonal ice have not been carried out to the same high order yet. However we do know from the first few terms of each that the same general appearance as that for cubic ice obtains. The coefficients are small, positive, and give the impression of relatively slow convergence.

To evaluate the pair correlation quantities from Eq. (5.72) both the numerator and denominator need to be expanded. The denominator is precisely the case just considered, excepting for the factor $(3/2)^N$. The numerator differs by inclusion of the distinguished vertices 1 and j, and consequently modified graph rules apply. For those numerator graphs an *odd* number (1 or 3) of bonds must terminate at the special vertices 1 and j, while even numbers (0,2,4) must terminate as before at the remaining N-2 vertices. The value that must be assigned to each numerator graph is (Gobush and Hoeve, 1972)

$$-(\lambda^n/3^{p_2+1})\,\mathbf{u}_1 \cdot \mathbf{u}_j \quad , \tag{5.76}$$

where $\mathbf{u}_1$ and $\mathbf{u}_j$ are unit vectors for the distinguished sites with directions determined by the vector sum of graph lines leaving those sites. As before n is the number of lines in the graph and p_2 is the number of order-two vertices.

Stillinger and Cotter (1973) evaluated the leading order terms of the series for first, second, and third coordination shell neighbors (j=2,3,4) in cubic ice. Their results were the following:

$$\langle \mu_1 \cdot \mu_2 \rangle / \langle \mu^2 \rangle = (\lambda/3) - 2(\lambda/3)^5 - 10(\lambda/3)^7 - 12(\lambda/3)^9 - 154(\lambda/3)^{11} - 1020(\lambda/3)^{13} + 0(\lambda^{15}) \quad ;$$

$$\langle \mu_1 \cdot \mu_3 \rangle / \langle \mu^2 \rangle = (1/3)(\lambda/3)^2 - 2(\lambda/3)^4 - 4(\lambda/3)^6 - 6(\lambda/3)^8 - 102(\lambda/3)^{10} - (1190/3)(\lambda/3)^{12} + 0(\lambda^{14}) \quad ;$$

$$\langle \mu_1 \cdot \mu_4 \rangle / \langle \mu^2 \rangle = -(2/3)(\lambda/3)^3 - (4/3)(\lambda/3)^5 - (14/3)(\lambda/3)^7 - 34(\lambda/3)^9 + 0(\lambda^{11}) \quad . \tag{5.77}$$

Corresponding expressions for more widely separated pairs have not been obtained, nor have any of the series for hexagonal ice due to more severe counting problems.

Stillinger and Cotter have compared the partial sums of increasing λ orders obtained from Eq. (5.77) for $\lambda = 1$ with the Monte Carlo estimates of the correlations calculated by Rahman and Stillinger (1972). They concluded that the series indeed converge to the simulation results. However the rates of convergence indicated by the known terms shown in Eq. (5.77) strongly indicated that $\lambda = 1$ was at the limit of convergence. When $|\lambda| < 1$ the corresponding partial sums appear to converge exponentially fast with increasing order. However when $\lambda = 1$ the convergence appears to go only algebraically (*i.e.* an inverse power) with increasing order. This observation is consistent with the previously mentioned suspicion that the configurational stiffness of the ice rules may be associated with long-range pair correlations (and indeed this was shown by Sutherland (1968) to be the case in square ice). For $|\lambda| < 1$ the presence of Bjerrum orientational defects limits correlation range by eliminating the stiffness, and it is a reasonable presumption that correlations are exponentially damped as distance increases. If this is the case then the exponential decay rate is probably simply related to the mean separation between Bjerrum defects, which goes continuously to infinity as λ approaches 1.

If indeed the pair correlations are exponentially damped when $|\lambda| < 1$ then the two quantities g and G will be identical:

$$g(\lambda) = G(\lambda) \qquad (|\lambda| < 1) \ . \tag{5.78}$$

However this equality need not obtain for $\lambda = 1$, since this appears to be a singular point. One or both of the functions could manifest a discontinuity at this singular point thus destroying the equality. This evidently is what has been observed for square ice in the Yanagawa-Nagle simulation study cited above. On account of the

qualitative similarity of all three ices it is reasonable to expect the same to occur in models of the cubic and hexagonal ices.

Separate correlation shell series such as those in Eq. (5.77) can be assembled (with due account given to coordination numbers) into series for $g(\lambda) = G(\lambda)$. This latter type of result was first obtained for cubic ice by Gobush and Hoeve (1972), and extended by Nagle (1974):

$$\begin{aligned} g(\lambda) = G(\lambda) = 1 &+ 4(\lambda/3) + 4(\lambda/3)^2 + 4(\lambda/3)^3 + 4(\lambda/3)^4 \\ &+ 4(\lambda/3)^5 - 4(\lambda/3)^6 - 12(\lambda/3)^7 + 36(\lambda/3)^8 \\ &+ 84(\lambda/3)^9 + 132(\lambda/3)^{10} + 292(\lambda/3)^{11} + 748(\lambda/3)^{12} \\ &+ 1124(\lambda/3)^{13} + 0(\lambda^{14}) \ , \qquad (|\lambda| < 1) \ . \end{aligned} \tag{5.79}$$

Once again numerical studies of the coefficients shown here seem to imply that the series converges at $\lambda = 1$ but that this is the limit of convergence.

It is instructive to examine the thirteenth-order polynomial $G_{13}(\lambda)$ defined by the first 14 terms in Eq. (5.79). This function is plotted in Figure 9. It is significant that this truncation of the full power series manages to pass through zero very close to $\lambda = -1$, where Eq. (5.68) states that G(-1) should vanish exactly. $G_{13}(\lambda)$ shows no marked sign of instability at this point, especially when compared to its lower-order analogs, so it seems safe to conclude that $G(\lambda)$ is continuous at $\lambda + -1$, with

$$\lim_{\lambda \to -1} G(\lambda) = 0 \ . \tag{5.80}$$

The polynomial $G_{13}(\lambda)$ should give an excellent approximation to the exact function $g(\lambda) = G(\lambda)$ when $|\lambda|$ is not too close to 1. In particular the monotonic increase with upward curvature displayed in Figure 9 is doubtless correct as λ approaches 1 from below. The indicated accelerating increase of overall correlation provides an

interesting contrast with the separate coordination shell functions exhibited earlier in Eq. (5.77). These latter functions show that beyond their respective leading terms, higher order corrections all have negative coefficients indicating negative correlation contributions as λ approaches 1. With the given $G(\lambda)$ behavior it is clear that as distant pairs develop predominately positive correlation they "feed off" the correlations already established at shorter range. Thus the developing configurational stiffness appears overall to displace positive correlation outward.

This last concept can be extended to offer an explanation of the difference between g and G that discontinuously develops when $\lambda = 1$. In particular we postulate that a weak non-decaying correlation inversely proportional to system size N suddenly arises at $\lambda = 1$, at the expense of short-range correlations. Specifically,

$$<\boldsymbol{\mu}_i \cdot \boldsymbol{\mu}_j>/<\mu^2> \sim K/N \qquad (\text{large } r_{ij};\ \lambda = 1) \tag{5.81}$$

where K may be dependent on the *direction* of $\mathbf{r}_{ij}$ relative to the principal lattice directions, but not on its magnitude. As Stillinger and Cotter (1973) have argued, this long-range phenomenon is precisely a reflection of the configurational stiffness that for $\lambda = 1$ locks together the polarizations of successive columns (square ice) or successive layers (cubic and hexagonal ice) of water molecules and causes them all to fluctuate together. In any case Eq. (5.81) implies

$$G(1) - g(1) = \overline{K} \ , \tag{5.82}$$

where $\overline{K}$ is the average of K over directions. If the long-range correlation given by K/N precisely represents a transfer of correlation from short range to long range, then only g will reflect that change and will have a jump discontinuity of negative magnitude at $\lambda = 1$. By contrast G would be continuous at $\lambda = 1$. That G should be continuous and g discontinuous, rather than both discontinuous, was a possibility first

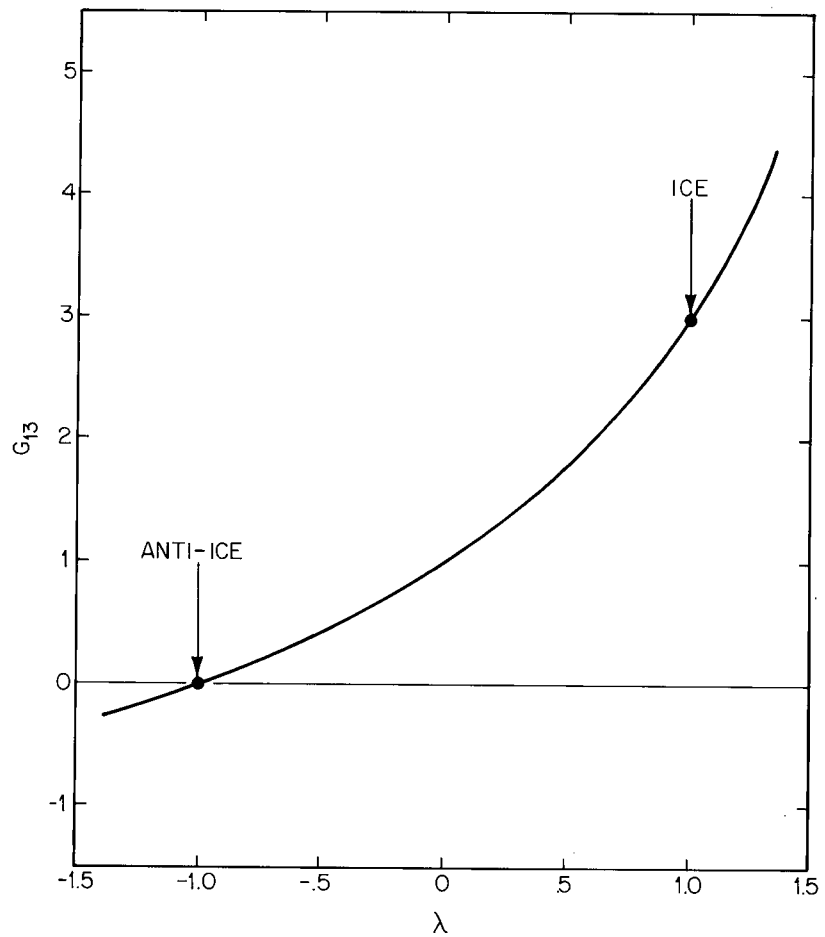

Figure 9. Plot of $G_{13}(\lambda)$, the sum of terms through thirteenth order from Eq. (5.79). This polynomial refers to cubic ice.

advanced by Nagle (1974). It is a presumption furthermore strongly supported by the Yanagawa-Nagle Monte Carlo study of square ice discussed above. For the three dimensional ices this implies that graph-theoretical results can reliably be employed to estimate G(1), and from the above we find for cubic ice specifically

$$G(1) \cong G_{13}(1) = 2.996\ 55\ldots \ . \tag{5.83}$$

The hexagonal ice value of G(1) ought to be closely similar, *i.e.* about 3.0 . By contrast with these G(1) values we have already cited substantially smaller values for g(1) from the Rahman-Stillinger Monte Carlo study, Eqs. (5.52) and (5.53).

Because the ice to anti-ice transformation changes the signs of correlations at every other relative lattice position, the weak non-decaying contribution (5.81) alternates from site to site when $\lambda = -1$. Consequently there will be overall cancellation and no contribution to $G(-1)$ as there is to $G(1)$. As a result we conclude that $G(-1)$ and $g(-1)$ are identical. In view of exact result (5.68) above we must then have

$$\lim_{\lambda \to -1} g(\lambda) = g(-1) = 0 \quad . \tag{5.84}$$

F. Discussion

The nearest-neighbor statistical models for ice thus far surveyed leave us with a basic dilemma. On the one hand the existence of Bjerrum defects in real ice requires λ in those models to be slightly less than 1, and that in turn implies $g(\lambda)$ and $G(\lambda)$ are equal. On the other hand the results (5.14) and (5.23) obtained from experimental data (processed respectively by the Kirkwood and by the Slater-Onsager equations) demand that

$$G/g \cong 2.54 \tag{5.85}$$

for ice at 0°C. This contradiction demands resolution and hence focusses attention on features of the ice problem that might be missing from the relatively simple nearest-neighbor models.

One obvious omission is the interaction between Bjerrum defects, already mentioned in passing. While the defects are charged [see Eq. (5.6)] they do not enjoy the complete mobility that would make them constitute an electrolyte. Instead they are

subject to statistical forces arising from the fact that their motion leaves a polarization field behind. Consequently the force acting between a pair of defects with charges q_1 and q_2 must be taken to be (Onsager and Dupuis, 1962):

$$\mathbf{F} = -q_1 q_2 \left(\frac{1}{\epsilon_\infty} + \frac{1}{\epsilon_0 - \epsilon_\infty} \right) \nabla \left(\frac{1}{r} \right) \quad . \tag{5.86}$$

Only the first term represents the standard Coulomb interaction. The net result of this modification is that test charges are incompletely shielded, as indeed one expects to observe in a dielectric medium, in contrast to a conductor. The distance over which this partial shielding can be expected to develop would be the cube root of defect concentration, or about 500 Å in ice near its melting point. The same dielectric shielding by interacting Bjerrum defects also applies to an embedded dipole.

The Slater-Onsager dielectric constant formula (5.20) was derived for ice in a slab geometry with conducting boundary conditions. It was argued that this eliminated at least the most important effects of long range dipolar interactions between molecules. The available theoretical estimates of G do not of course use conducting boundary conditions but the more convenient periodic boundary conditions. However this distinction is not usually regarded as a source of error by those concerned with such matters. Since use of the conducting boundary is likewise presumed to remove shape dependence of G from the problem, then the theoretical calculations of G ought to give results equally applicable to both slabs and spheres of ice surrounded by conducting boundaries.

For a sphere of ice composed of polarizable molecules and surrounded by a conductor it is a simple matter to adapt Kirkwood's argument (Kirkwood, 1939), originally devised for a sphere *in vacuo*, to show that the local moment $g\langle\mu^2\rangle^{1/2}$ and the corresponding overall moment $G\langle\mu^2\rangle^{1/2}$ must be in the ratio

$$G/g = 3\epsilon_0/(2\epsilon_0 + 1) \ , \qquad (5.87)$$

in other words about 1.5 . This argument of course treats the ice medium as a proper dielectric, and for that reason interacting Bjerrum defects are implicitly invoked. Although this conclusion explains part of the discrepancy between G and g, it does not yield the ratio 2.54 . It might be worth mentioning in passing that no reasonable alternative value for ϵ_∞ can rectify matters, nor can introduction of any reasonable ϕ in the Kirkwood equation do likewise.

We are left with the necessity for extending the present nearest-neighbor statistical theory of ice to include at least interacting Bjerrum defects. Furthermore it seems important to check whether those extended models indeed exhibit the insensitivity to boundary conditions assumed above, namely that G should be the same for (a) periodic boundary conditions, (b) slab geometry with surrounding conductor, and (c) spherical geometry with surrounding conductor. In the present incomplete and therefore unsatisfactory state of the subject it appears likely these assumptions may require revision.

VI. CONCLUSION

This review constitutes an interim report for the subject of low frequency dielectric response in liquid and solid water. While many of the basic concepts are reasonably well understood there remain important issues that require further research. In the liquid phase, the quantities $<\mu^2>^{1/2}$, g, and ϕ each need to be characterized quantitatively. In ice $<\mu^2>^{1/2}$ similarly needs to be determined accurately, and the apparent contradiction between theoretical and experimental values for G/g must be resolved. At least part of the missing information can best be supplied by realistic computer simulation studies of water in its condensed phases, with proper attention paid to molecular polarizability.

REFERENCES

Akerlof, G. C. and Oshry, H. J. (1950). "The Dielectric Constant of Water at High Temperatures and in Equilibrium with its Vapor." *J. Am. Chem. Soc.* **72,** 2844-2847.

Auty, R. P. and Cole, R. H. (1952). "Dielectric Properties of Ice and Solid D_2O." *J. Chem. Phys.* **20,** 1309-1314.

Bernal, J. D. and Fowler, R. H. (1933). "A Theory of Water and Ionic Solution, With Particular Reference to Hydrogen and Hydroxyl Ions." *J. Chem. Phys.* **1,** 515-548.

Bjerrum, N. (1952). "Structure and Properties of Ice." *Science* **115,** 385-390.

Buckingham, A. D. (1956). A Theory of the Dielectric Polarization of Polar Substances." *Proc. R. Soc.*, **A, 238,** 235-244.

Del Bene, J. and Pople, J. A. (1970). "Theory of Molecular Interactions. I. Molecular Orbital Studies of Water Polymers Using a Minimal Slater-Type Basis." *J. Chem. Phys.* **52,** 4858-4866.

Del Bene, J. E. and Pople, J. A. (1973). "Theory of Molecular Interactions. III. A Comparison of Studies of H_2O Polymers Using Different Molecular-Orbital Basis Sets." *J. Chem. Phys.* **58,** 3605-3608.

DiMarzio, E. A. and Stillinger, F. H. (1964). "The Residual Entropy of Ice." *J. Chem. Phys.* **40,** 1577-1581.

Dyke, T. R., Mack, K. M., and Muenter, J. S. (1977). "The Structure of Water Dimer from Molecular Beam Electric Resonance Spectroscopy." *J. Chem. Phys.* **66,** 498-510.

Dyke, T. R. and Muenter, J. S. (1973). "Electric Dipole Moments of Low J States of H_2O and D_2O." *J. Chem. Phys.* **59,** 3125-3127.

Eisenberg, D. and Kauzmann, W. (1969). *The Structure and Properties of Water.* Oxford University Press, New York. p. 15.

Fletcher, N. H. (1970). *The Chemical Physics of Ice,* Cambridge University Press, Cambridge. p. 156.

Franck, E. U. (1970). "Water and Aqueous Solutions at High Pressures and Temperatures." *Pure Appl. Chem.* **24,** 13-30.

Geiger, A., Stillinger, F. H., and Rahman, A. (1979). "Aspects of the Percolation Process for Hydrogen-Bond Networks in Water." *J. Chem. Phys.* **70,** 4185-4193.

Giaque, W. F. and Stout, J. W. (1936). "The Entropy of Water and the Third Law of Thermodynamics. The Heat Capacity of Ice from 15° to 273°K." *J. Amer. Chem. Soc.* **58,** 1144-1150.

Gobush, W., Jr., and Hoeve, C. A. J. (1972). "Calculation of the Dielectric Correlation Factor of Cubic Ice." *J. Chem. Phys.* **57,** 3416-3421.

Hankins, D., Moskowitz, J. W., and Stillinger, F. H. (1970). "Water Molecule Interactions." *J. Chem. Phys.* **53,** 4544-4554.

Hankins, D., Moskowitz, J. W., and Stillinger, F. H. (1973). "Erratum: Water Molecule Interactions." *J. Chem. Phys.* **59,** 995.

Harris, F. E. and Alder, B. J. (1953). "Dielectric Polarization of Polar Substances." *J. Chem. Phys.* **21,** 1031-1038.

Hasted, J. B. (1973). *Aqueous Dielectrics,* Chapman and Hall, London.

Hodge, I. M. and Angell, C. A. (1978). "The Relative Permittivity of Supercooled Water." *J. Chem. Phys.* **68,** 1363-1368.

Humbel, F., Jona, F., and Scherrer, P. (1953). "Anisotropie der Dielektrizitätskonstante des Eises." *Helv. Phys. Acta* **26,** 17-32.

Irvine, W. M. and Pollack, J. B. (1968). "Infrared Optical Properties of Water and Ice Spheres." *Icarus* **8,** 324-360.

Jeffrey, G. A. (1969). "Water Structure in Organic Hydrates," *Accts. Chem. Res.* **2,** 344-352.

Johari, G.P. and Jones, S.J. (1978). *J. Glaciology,* 21, 259.

Kanno, H. and Angell, C. A. (1979). "Water: Anomalous Compressibilities to 1.9 kbar and Correlation with Supercooling Limits," *J. Chem. Phys.* **70,** 4008-4016.

Kavanau, J. L. (1964). *Water and Solute-Water Interactions.* Holden-Day, San Francisco, pp. 10-14.

Kern, C. W. and Karplus, M. (1972). "The Water Molecule," in *Water, A Comprehensive Treatise,* Vol. 1 (ed. F. Franks), Plenum, New York, pp. 21-91.

Kirkwood, J. G. (1939). "The Dielectric Polarization of Polar Liquids," *J. Chem. Phys.* **7,** 911-919.

Kittel, C. (1958). *Elementary Statistical Physics,* Wiley, New York, pp. 206-210.

Kramers, H. A. and Wannier, G. H. (1941). "Statistics of the Two-Dimensional Ferromagnet, Part I," *Phys. Rev.* **60,** 252-262.

Lentz, B. R. and Scheraga, H. A. (1973). "Water Molecule Interactions. Stability of Cyclic Polymers," *J. Chem. Phys.* **58,** 5296-5308.

Levi, L., Milman, O., and Suraski, E. (1963). "Electrical Conductivity and Dissociation Constants in Ice Doped with HF and NH_3 in Different Ratios," *Trans. Faraday Soc.* **59,** 2064-2075.

Lieb, E. H. (1967a). "Exact Solution of the Problem of the Entropy of Two-Dimensional Ice," *Phys. Rev. Letters* **18,** 692-694.

Lieb, E. H. (1967b). "Residual Entropy of Square Ice," *Phys. Rev.* **162,** 162-171.

Lieb, E. H. and Wu, F. Y. (1972). "Two-Dimensional Ferroelectric Models," in *Phase Transitions and Critical Phenomena,* Vol. 1, edited by C. Domb and M. S. Green (Academic Press, New York), pp. 331-490.

Liebmann, S. P. and Moskowitz, J. W. (1971). Polarizabilities and Hyperpolarizabilities of Small Polyatomic Molecules in the Uncoupled Hartree-Fock Approximation. *J. Chem. Phys.* **54,** 3622-3631.

Malmberg, C. G. (1958). "Dielectric Constant of Deuterium Oxide," *J. Res. NBS* **60,** 609-612.

Malmberg, C. G. and Maryott, A. A. (1956). "Dielectric constant of Water from 0° to 100°. *J. Res. NBS* **56,** 1-8.

Meijering, J. L. (1957). "Residual Entropy of Ice, and Related Combinatorial Problems," *Philips Res. Rep.* **12,** 333-350.

Nagle, J. F. (1966). "Lattice Statistics of Hydrogen Bonded Crystals. I. The Residual Entropy of Ice," *J. Math. Phys.* **7,** 1484-1491.

Nagle, J. F. (1968). "Weak-Graph Method for Obtaining Formal Series Expansions for Lattice Statistical Problems," *J. Math. Phys.* **9,** 1007-1019.

Nagle, J. F. (1974). "Dielectric Constant of Ice," *J. Chem. Phys.* **61,** 883-888.

Nagle, J. F. (1979). "Theory of the Dielectric Constant of Ice," *Chem. Physics,* **43,** 317-328.

Narten, A. H., Venkatesh, C. G., and Rice, S. A. (1976). "Diffraction Pattern and Structure of Amorphous Solid Water at 10 and 77°K," *J. Chem. Phys.* **64,** 1106-1121.

Olovsson, I. and Jönsson, P.-G. (1975). "X-ray and Neutron Diffraction Studies of Hydrogen Bonded Systems," in *The Hydrogen Bond. II. Structure and Spectroscopy* (ed. P. Schuster, G. Zundel, and C. Sandorfy, North-Holland, New York), pp. 393-456.

Onsager, L. (1967). "Ferroelectricity in Ice?" in *Ferroelectricity* (ed. E. F. Weller), Elsevier, Amsterdam, pp. 16-19.

Onsager, L. (1973). "Introductory Lecture," in *Physics and Chemistry of Ice* (ed. E. Whalley, S. J. Jones, and L. W. Gold), Royal Soc. of Canada, Ottawa, pp. 7-12.

Onsager, L. and Dupuis, M. (1960). "The Electrical Properties of Ice." Rend. Scuola Intern. Fis. "Enrico Fermi," X Corso, 294-315.

Onsager, L. and Dupuis, M. (1962). "The Electrical Properties of Ice," in *Electrolytes,* ed. B. Pesce, Pergamon Press, Oxford, pp. 27-46.

Owen, B. B., Miller, R. C., Milner, C. E., and Cogan, H. L. (1961). "The Dielectric Constant of Water as a Function of Temperature and Pressure," *J. Phys. Chem.* **65,** 2065-2070.

Pauling, L. (1935). "The Structure and Entropy of Ice and Other Crystals with Some Randomness of Atomic Arrangement," *J. Amer. Chem. Soc.* **57,** 2680-2684.

Peterson, S. W. and Levy, H. A. (1957). "A Single-Crystal Neutron Diffraction Study of Heavy Ice," *Acta Cryst.* **10,** 70-76.

Pople, J. A. (1951). "Molecular Association in Liquids. II. A Theory of the Structure of Water," *Proc. R. Soc.* **A, 205,** 163-178.

Querry, M. R., Curnutte, B., and Williams, D. (1969). "Refractive Index of Water in the Infrared," *J. Opt. Soc. Amer.* **59,** 1299-1305.

Rahman, A. and Stillinger, F. H. (1972). "Proton Distribution in Ice and the Kirkwood Correlation Factor," *J. Chem. Phys.* **57,** 4009-4017.

Rahman, A. and Stillinger, F. H. (1973). "Hydrogen-Bond Patterns in Liquid Water," *J. Amer. Chem. Soc.* **95,** 7943-7948.

Slater, J. C. (1941). "Theory of the Transition in KH_2PO_4," *J. Chem. Phys.* **9,** 16-33.

Speedy, R. J. and Angell, C. A. (1976). "Isothermal Compressibility of Supercooled Water and Evidence for a Thermodynamic Singularity at -45°C. *J. Chem. Phys.* **65,** 851-858.

Stanley, H. E. (1971). *Introduction to Phase Transitions and Critical Phenomena.* Oxford University Press, New York.

Stillinger, F. H. (1970). "Effective Pair Interactions in Liquids Water," *J. Phys. Chem.* **74,** 3677-3687.

Stillinger, F. H. (1975). "Theory and Molecular Models for Water," in *Advances in Chemical Physics,* Vol. XXXI (ed. I. Prigogine and S. Rice), Wiley-Interscience, New York, pp. 1-101.

Stillinger, F. H. (1977). "Theoretical Approaches to the Intermolecular Nature of Water," *Phil. Trans. R. Soc. Lond.* **B, 278,** 97-110.

Stillinger, F. H. (1978). "Proton Transfer Reactions and Kinetics in Water," in *Theoretical Chemistry, Advances and Perspectives,* Vol. 3, (ed. H. Eyring and D. Henderson), Academic Press, New York, pp. 177-234.

Stillinger, F. H. and Cotter, M. A. (1973). "Local Orientational Order in Ice," *J. Chem. Phys.* **58,** 2532-2541.

Stillinger, F. H. and David, C. W. (1978). "Polarization Model for Water and Its Dissociation Products," *J. Chem. Phys.* **69,** 1473-1484.

Stillinger, F. H. and Lemberg, H. L. (1975). "Symmetry Breaking in Water Molecule Interactions," *J. Chem. Phys.* **62,** 1340-1346.

Stillinger, F. H. and Rahman, A. (1974). "Improved Simulation of Liquid Water," *J. Chem. Phys.* **60,** 1545-1557.

Sutherland, B. (1968). "Correlation Functions for Two-Dimensional Ferroelectrics," *Phys. Letters* **26A,** 532-533.

Sutherland, B., Yang, C. N., and Yang, C. P. (1967). "Exact Solution of a Model of Two-Dimensional Ferroelectrics in an Arbitrary External Electric Field," *Phys. Rev. Letters* **19,** 588-591.

Van Thiel, M., Becker, E. D., and Pimentel, G. C. (1957). "Infrared Studies of Hydrogen Bonding of Water by the Matrix Isolation Technique," *J. Chem. Phys.* **27,** 486-490.

Verhoeven, J. and Dymanus, A. (1970). "Magnetic Properties and Molecular Quadrupole Tensor of the Water Molecule by Beam-Maser Zeeman Spectroscopy," *J. Chem. Phys.* **52,** 3222-3233.

Wörz, O. and Cole, R. H. (1969). "Dielectric Properties of Ice I.," *J. Chem. Phys.* **51,** 1546-1551.

Yanagawa, A. (1979). "Calculations of Correlation Functions for Two-Dimensional Square Ice," Ph.D. thesis, Carnegie-Mellon Univ., Pittsburgh.

Yanagawa, A. and Nagle, J. F. (1979). "Calculations of correlation Functions for Two-dimensional Square Ice," *Chem. Physics* **43,** 329-339.

Eq. (4.25):

replace $\mu_{\nu 1} \cdot \mu_{\nu 2}$ by $\mu_{\nu 1} \mu_{\nu 2}$

p. 369: although $M_{\nu 1}$ in principle

Eq. (12.23): 10^{-18} esu cm

CORRECTIONS